Selective inhibition of prolyl 4-hydroxylases by bipyridinedicarboxylates

James D. Vasta and Ronald T. Raines*

Section	Contents	Page
I	HPLC Chromatograms	S2
II	NMR Spectra	S17
III	Absorption Spectra of Bipyridine Ligands and Their Complexes with Fe(II)	S32
IV	Plots of Fe(II) Binding by Bipyridine Ligands	S36
V	Job Plots of Fe(II) Binding by Bipyridine Ligands	S39
VI	Dose–Response Curve for Inhibition of Human CP4H1 by Compound **4b**	S42

I. HPLC Chromatograms

3-Methoxycarbonylpyridine *N*-oxide

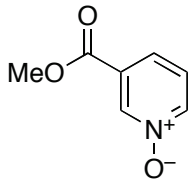

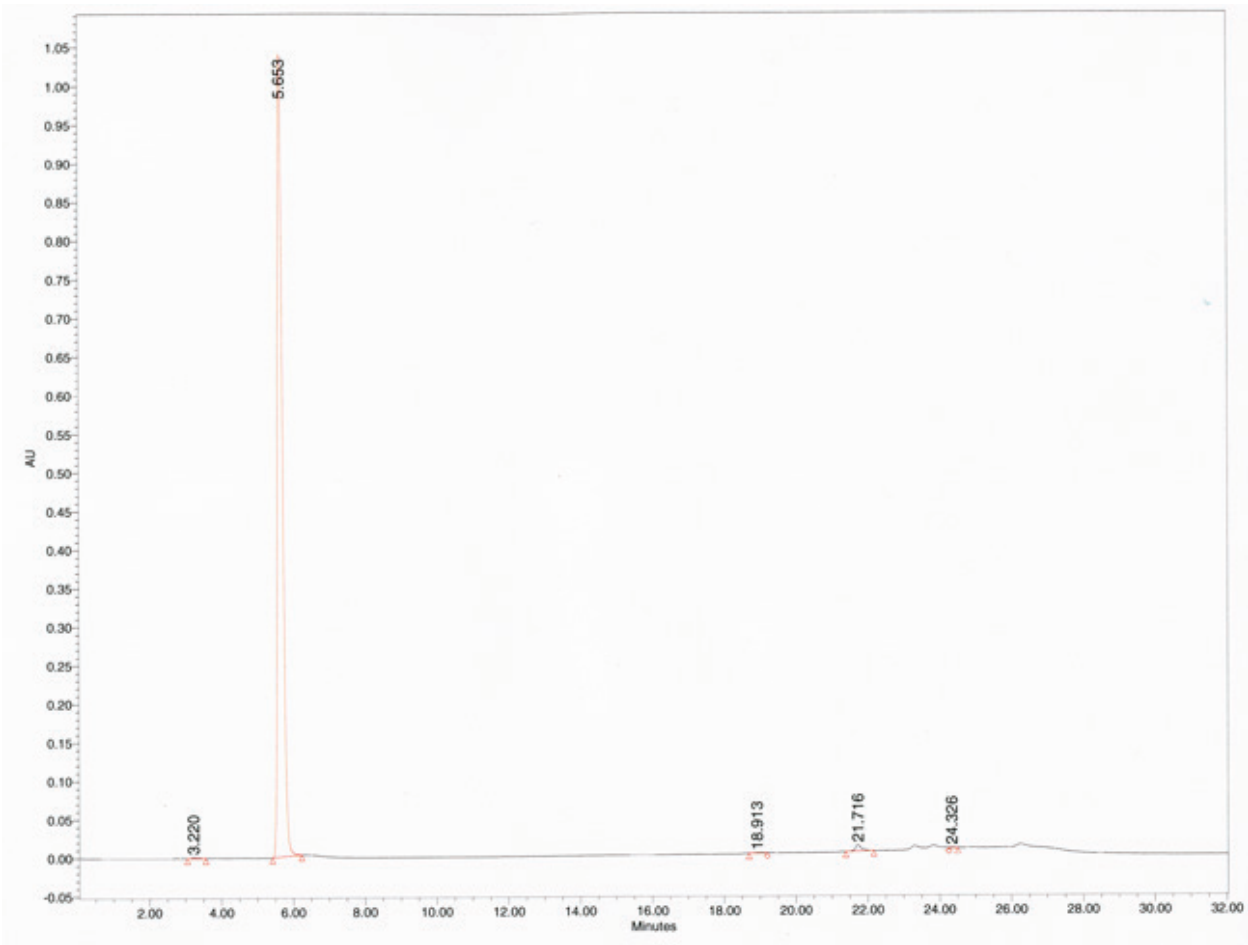

Peak	Retention Time (min)	Area (μV·s)	% Area	Height (μV)
1	3.22	13456	0.13	1356
2	**5.653**	**10173512**	**98.71**	**1045398**
3	18.913	13293	0.13	623
4	21.716	98669	0.96	8309
5	24.326	7021	0.07	858

4-Methoxycarbonylpyridine *N*-oxide

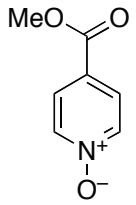

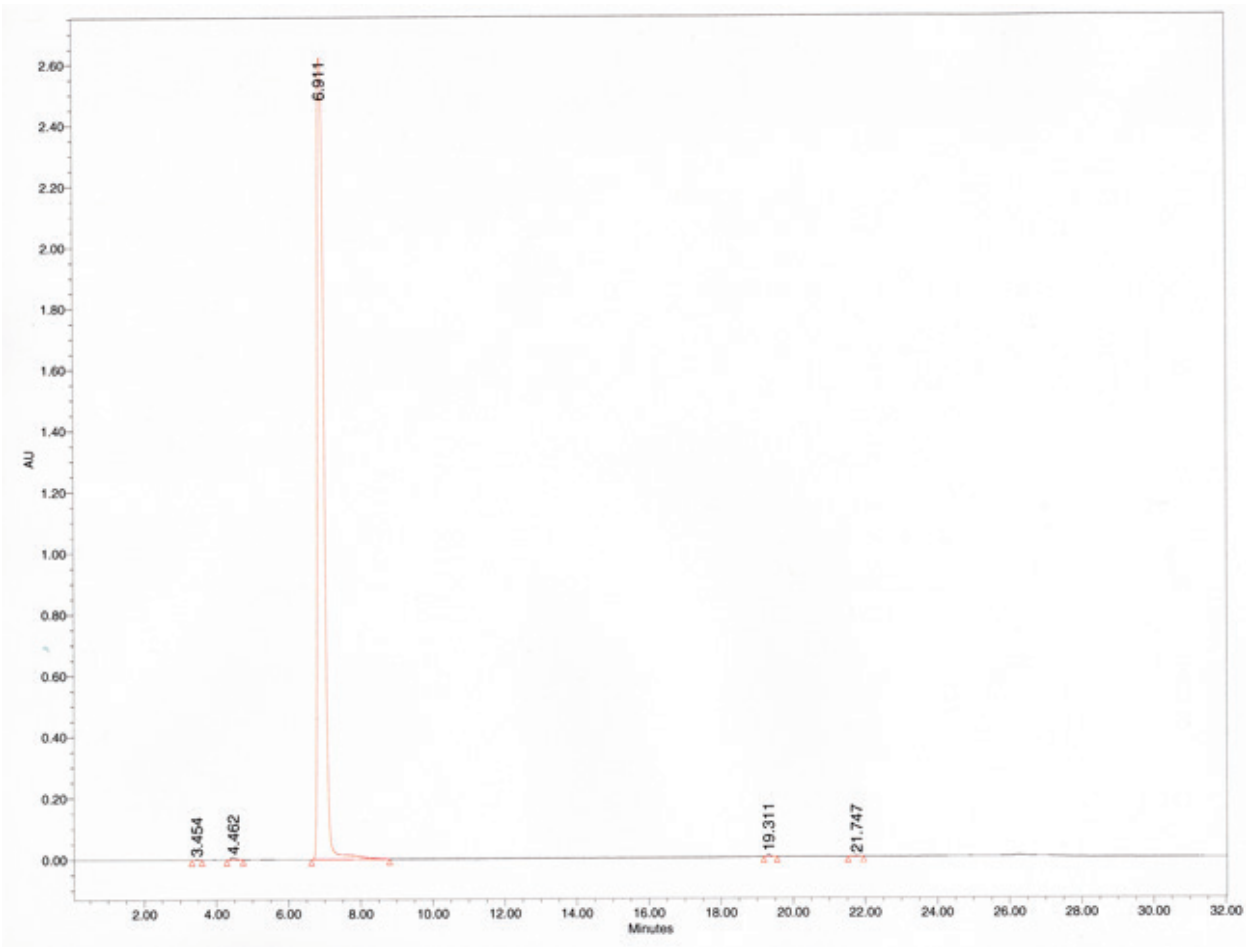

Peak	Retention Time (min)	Area (μV·s)	% Area	Height (μV)
1	3.454	6669	0.02	1148
2	4.462	68515	0.2	8176
3	**6.911**	**33472343**	**99.59**	**2623673**
4	19.311	48585	0.14	7532
5	21.747	14944	0.04	1754

5-Methoxycarbonyl-2-(4-methoxycarbonylpyridin-2-yl)pyridine *N*-oxide

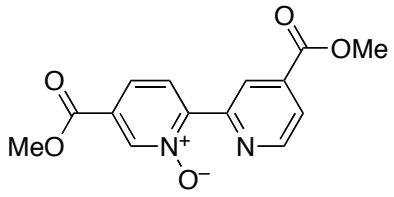

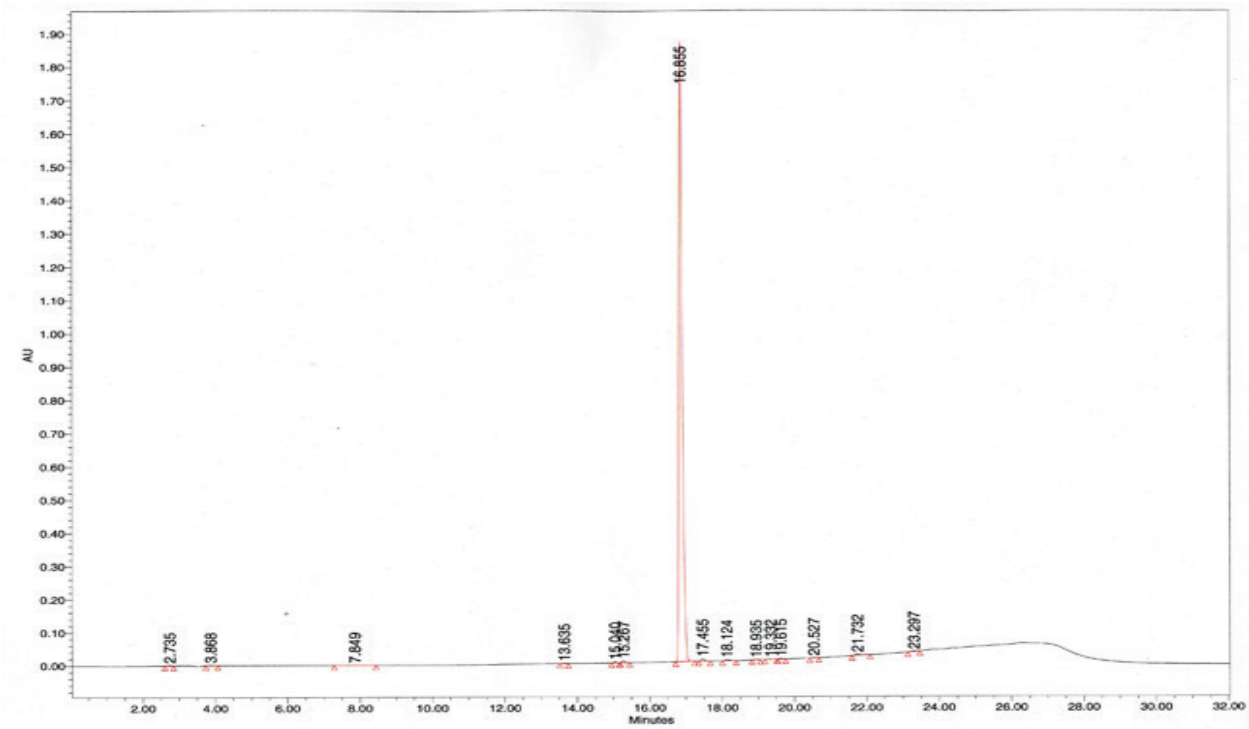

Peak	Retention Time (min)	Area (μV·s)	% Area	Height (μV)
1	2.735	13037	0.11	2049
2	3.868	10779	0.09	1071
3	7.849	13882	0.11	369
4	13.635	2026	0.02	299
5	15.04	17327	0.14	3104
6	15.267	34877	0.29	6078
7	**16.855**	**11901432**	**98.04**	**1885885**
8	17.455	46443	0.38	7399
9	18.124	30013	0.25	3621
10	18.935	3385	0.03	509
11	19.332	4940	0.04	618
12	19.615	6866	0.06	1127
13	20.527	5029	0.04	707
14	21.732	39489	0.33	3867
15	23.297	9688	0.08	912

4-Methoxycarbonyl-2-(6-methoxycarbonylpyridin-2-yl)pyridine *N*-oxide

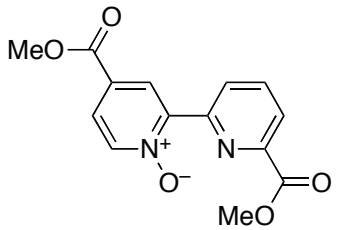

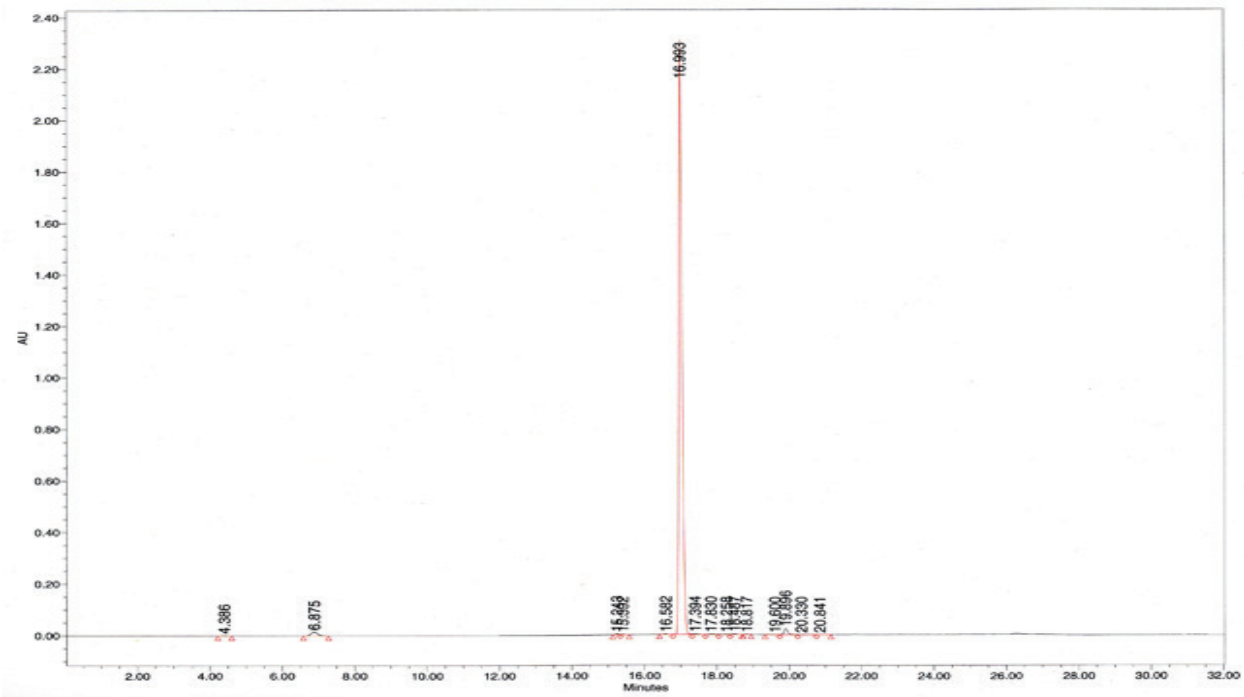

Peak	Retention Time (min)	Area (μV·s)	% Area	Height (μV)
1	4.386	5642	0.04	563
2	6.875	180530	1.24	14393
3	15.243	21025	0.14	3817
4	15.392	9202	0.06	1524
5	16.582	10787	0.70	1507
6	**16.993**	**14068452**	**96.75**	**2291477**
7	17.394	13684	0.09	1587
8	17.83	11710	0.08	1477
9	18.258	8340	0.06	869
10	18.487	18806	0.13	2734
11	18.817	6780	0.05	1180
12	19.6	3606	0.02	276
13	19.896	176578	1.21	24395
14	20.33	2324	0.02	288
15	20.841	3094	0.02	314

5-Methoxycarbonyl-2-(6-methoxycarbonylpyridin-2-yl)pyridine *N*-Oxide

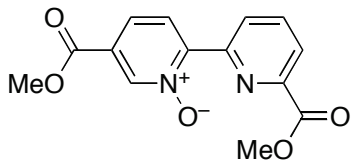

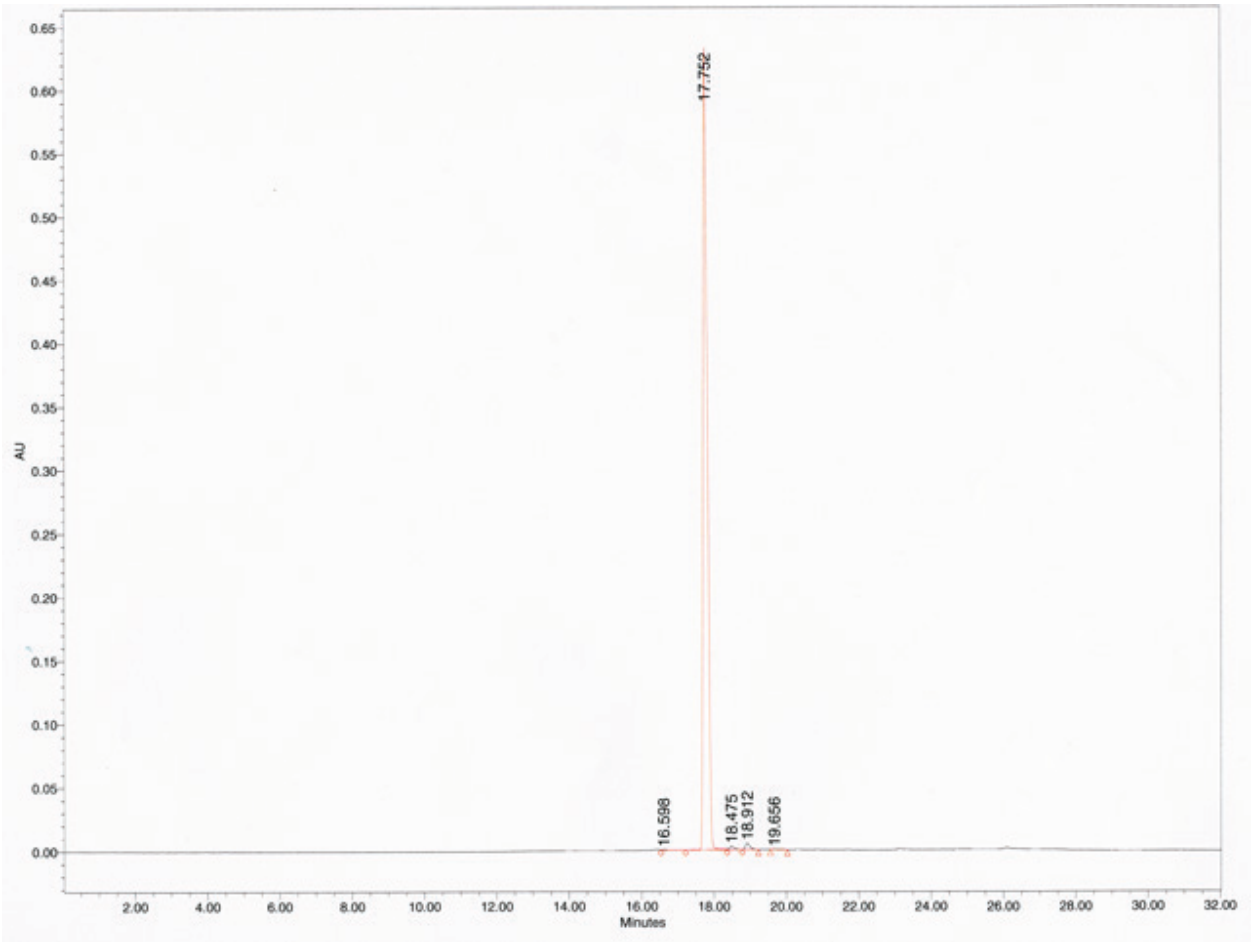

Peak	Retention Time (min)	Area (μV·s)	% Area	Height (μV)
1	16.598	5066	0.10	390
2	**17.752**	**5074068**	**98.50**	**630451**
3	18.475	24831	0.48	2622
4	18.912	43364	0.84	4994
5	19.656	4232	0.80	320

Dimethyl 2,2′-bipyridine-4,5′-dicarboxylate

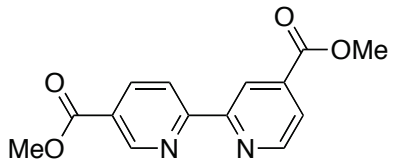

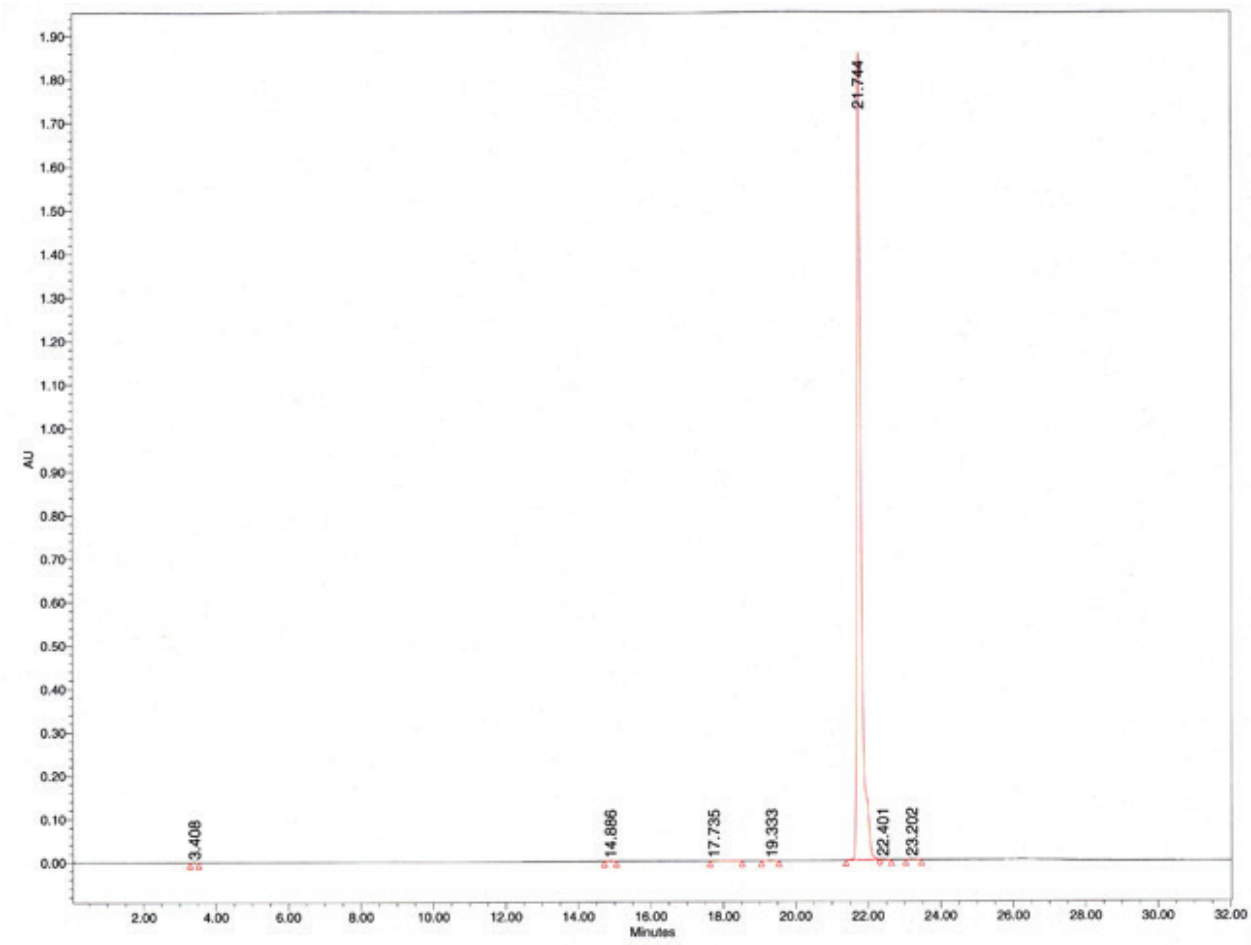

Peak	Retention Time (min)	Area (μV·s)	% Area	Height (μV)
1	3.408	2855	0.02	480
2	14.886	6487	0.04	971
3	17.735	5271	0.04	342
4	19.333	5392	0.04	454
5	**21.744**	**14975268**	**99.65**	**1855605**
6	22.401	15565	0.10	2001
7	23.202	17522	0.12	1973

Dimethyl 2,2′-bipyridine-4,6′-dicarboxylate

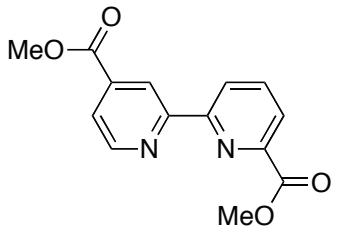

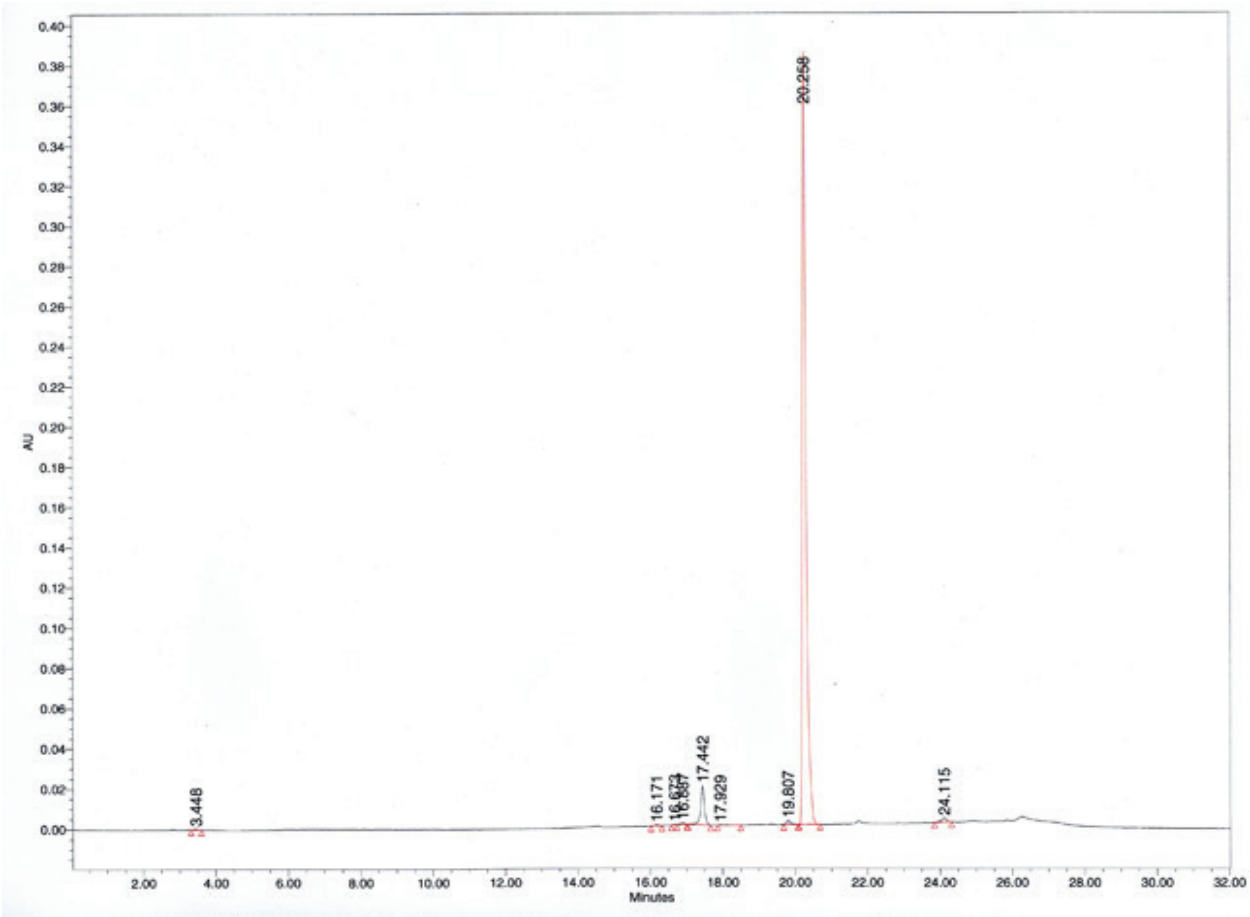

Peak	Retention Time (min)	Area (μV·s)	% Area	Height (μV)
1	3.448	2487	0.09	430
2	16.171	3810	0.13	502
3	16.673	921	0.03	214
4	16.887	5841	0.20	876
5	17.442	143408	5.01	19470
6	17.929	3204	0.11	246
7	19.807	15865	0.55	2039
8	**20.258**	**2663252**	**93.12**	**382022**
9	24.115	21169	0.74	2136

Dimethyl 2,2′-bipyridine-4,6′-dicarboxylate

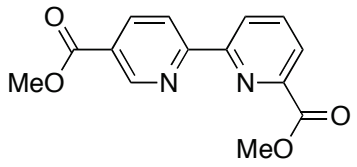

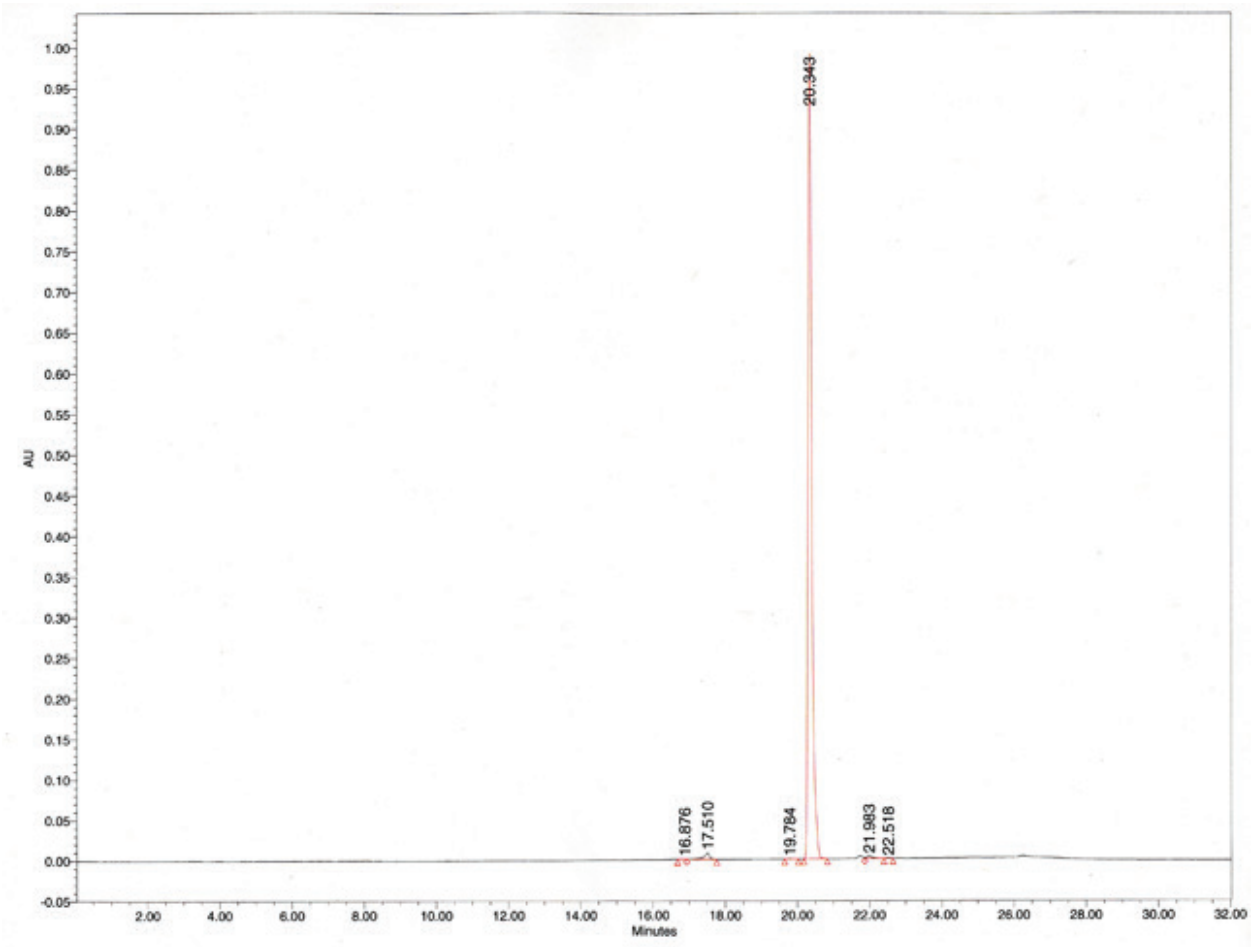

Peak	Retention Time (min)	Area (μV·s)	% Area	Height (μV)
1	16.876	3500	0.05	327
2	17.51	91422	1.26	7940
3	19.784	3681	0.05	418
4	**20.343**	**7113302**	**98.13**	**985946**
5	21.983	32924	0.45	3450
6	22.518	3734	0.05	574

2,2′-Bipyridine-4,5′-dicarboxylic acid (4c)

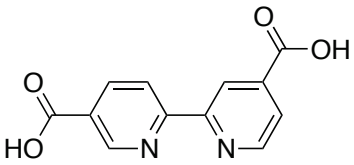

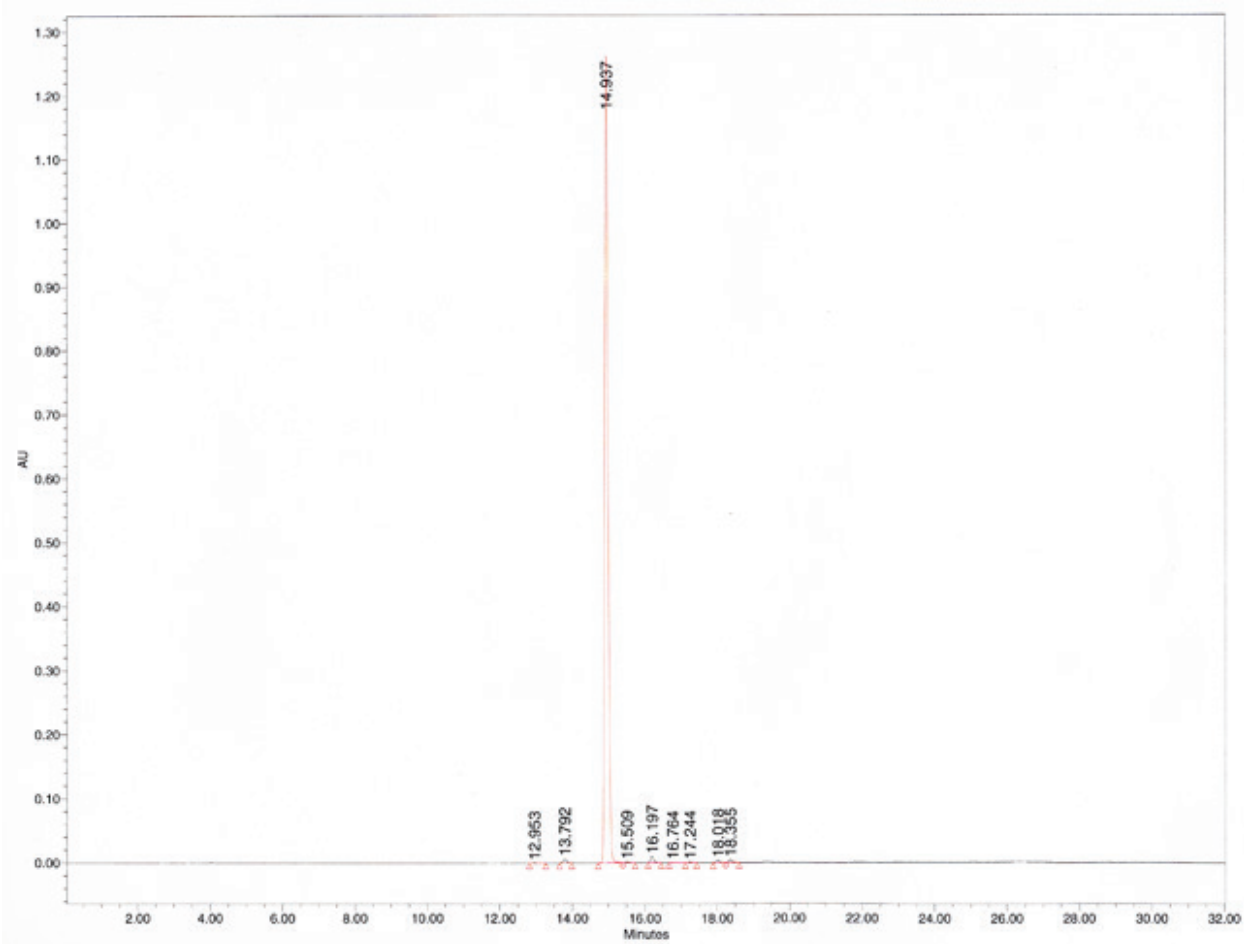

Peak	Retention Time (min)	Area (μV·s)	% Area	Height (μV)
1	12.953	2349	0.03	342
2	13.792	41201	0.50	6230
3	**14.937**	**8057213**	**97.81**	**1275038**
4	15.509	9592	0.12	1195
5	16.197	59429	0.72	9616
6	16.764	4174	0.05	384
7	17.244	6066	0.07	927
8	18.018	25356	0.31	3755
9	18.355	32573	0.40	4703

2,2′-Bipyridine-4,6′-dicarboxylic acid (4d)

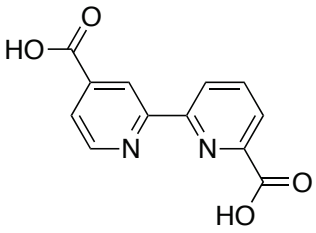

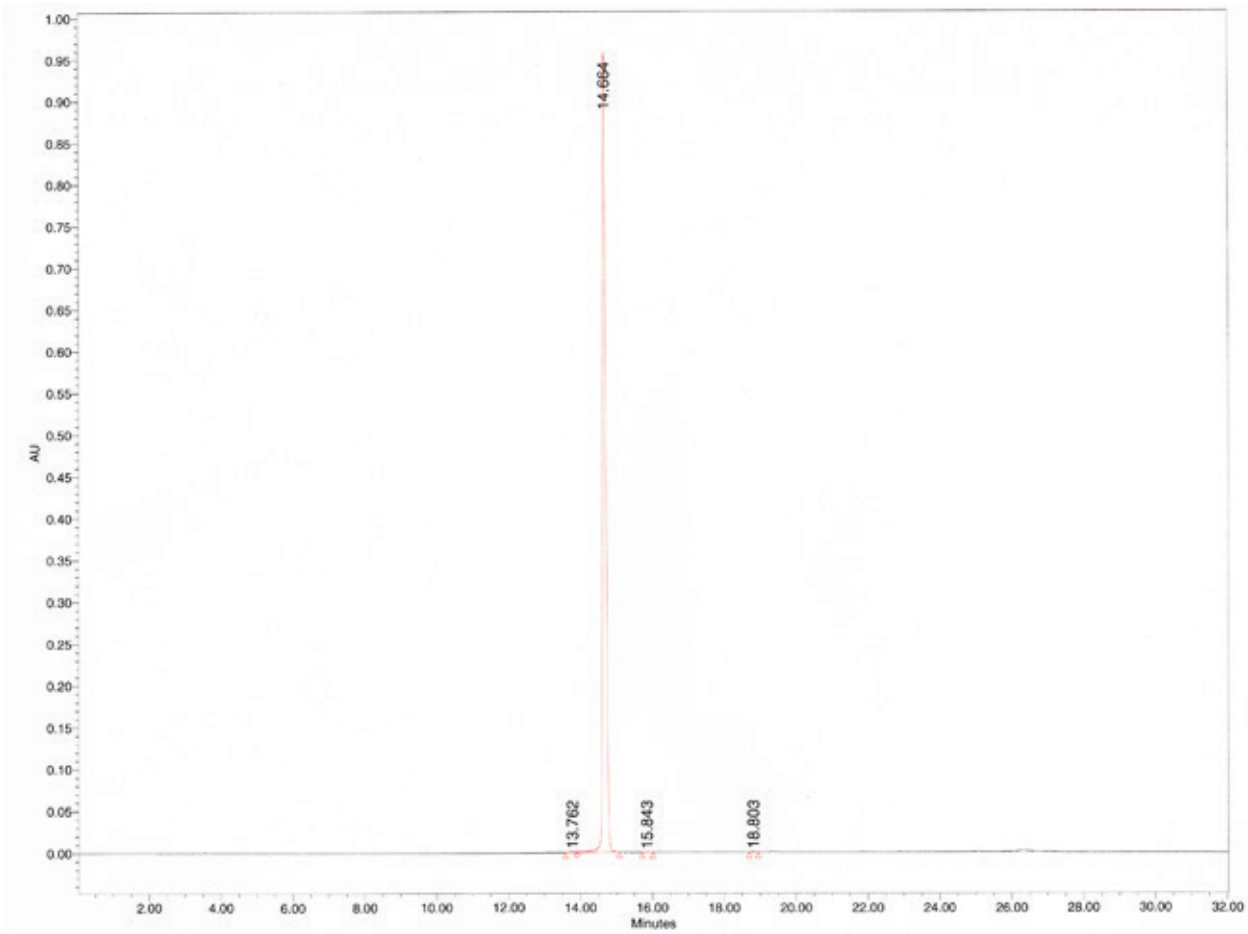

Peak	Retention Time (min)	Area (μV·s)	% Area	Height (μV)
1	13.762	7264	0.12	768
2	**14.664**	**5934760**	**99.8**	**962317**
3	15.843	1879	0.03	305
4	18.803	2797	0.05	481

2,2′-Bipyridine-5,6′-dicarboxylic acid (4f)

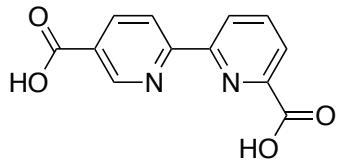

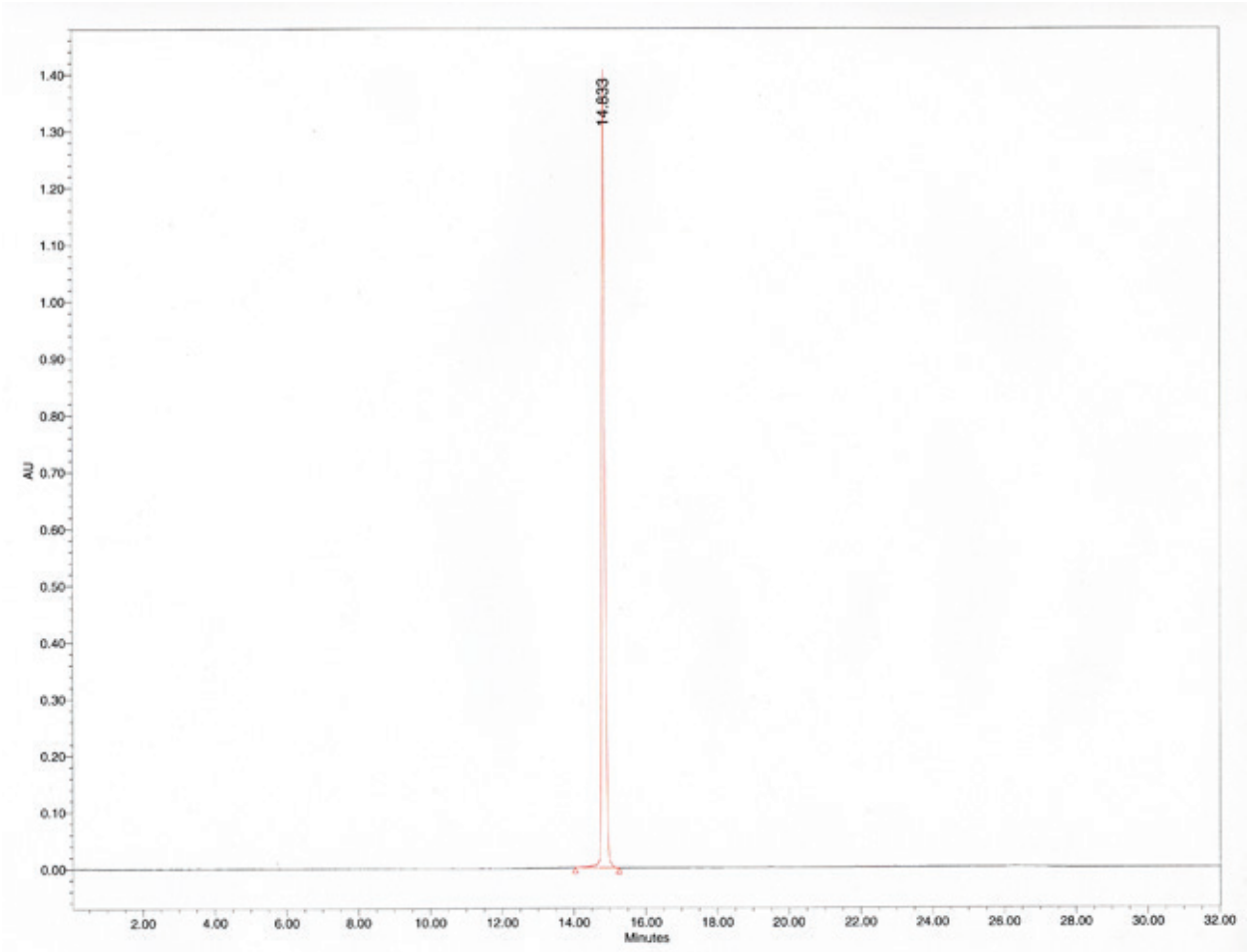

Peak	Retention Time (min)	Area (μV·s)	% Area	Height (μV)
1	**14.833**	**8630006**	**100**	**962317**

***N*-(Methoxyoxalyl)glycine ethyl ester**

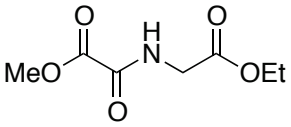

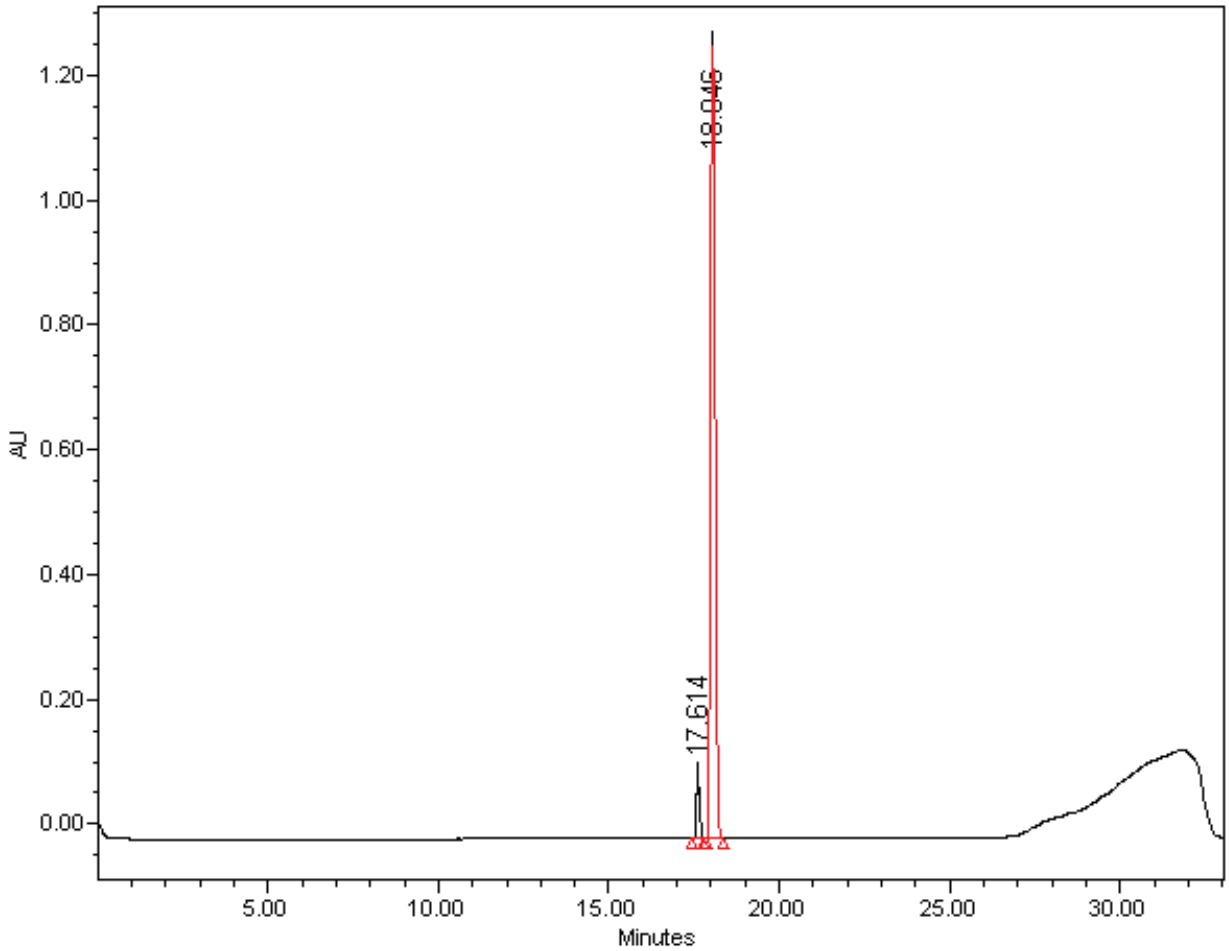

Peak	Retention Time (min)	Area (mV·s)	% Area	Height (mV)
1	17.614	678345	5.32	97875
2	**18.046**	**12072069**	**94.68**	**1271789**

***N*-Oxalylglycine (2)**

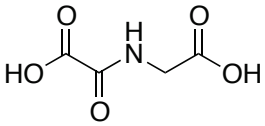

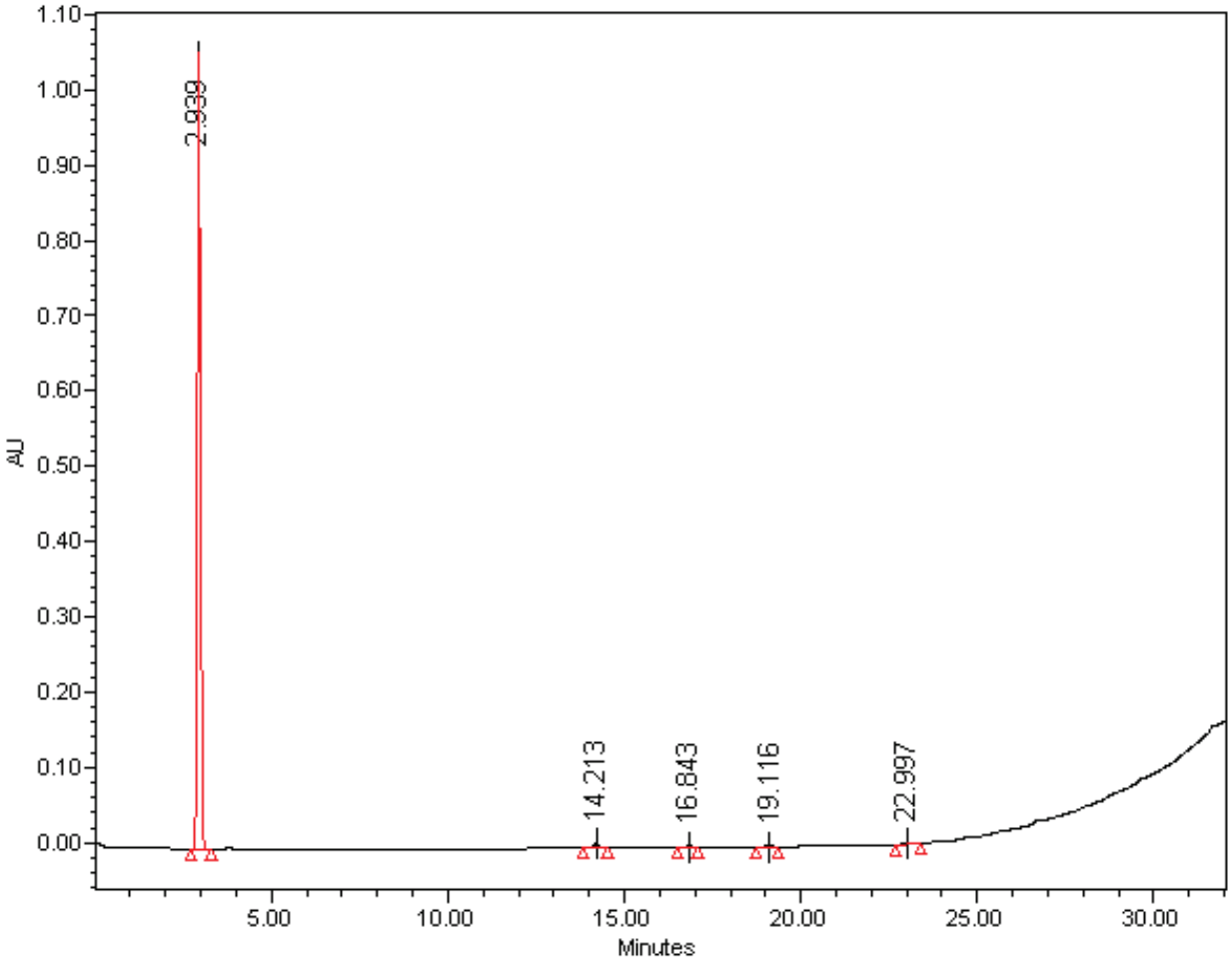

Peak	Retention Time (min)	Area (mV·s)	% Area	Height (mV)
1	**2.939**	**6423296**	**98.12**	**1052708**
2	14.213	45684	0.7	6442
3	16.843	18876	0.29	1754
4	19.116	14825	0.23	733
5	22.997	43535	0.67	2475

Cbz-Pro-Pro-Gly-OEt

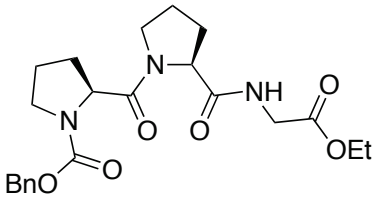

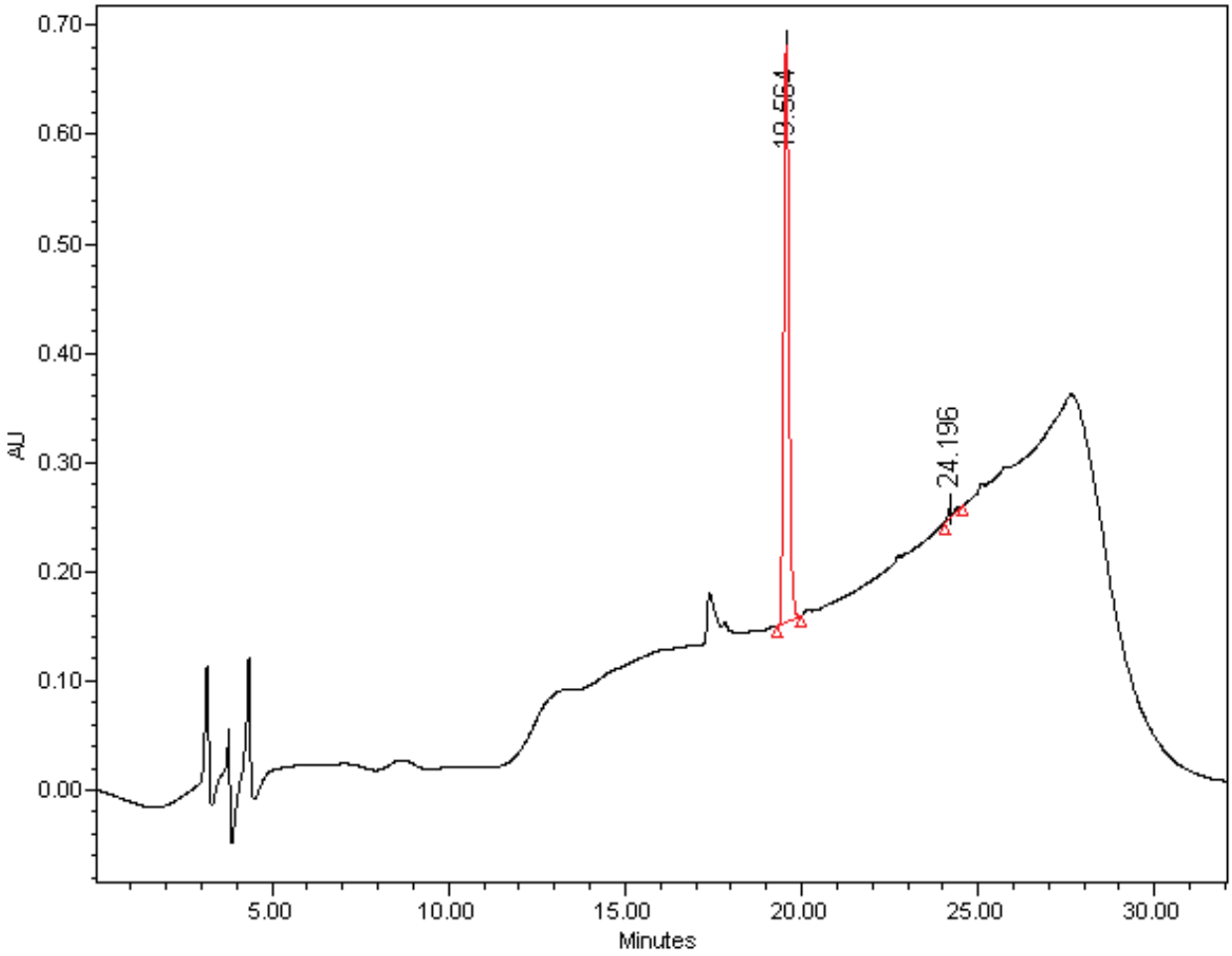

Peak	Retention Time (min)	Area (μV·s)	% Area	Height (μV)
1	19.564	5386891	98.50	527526
2	**24.196**	**81974**	**1.50**	**8342**

Dansyl-Gly-Pro-Pro-Gly-OEt

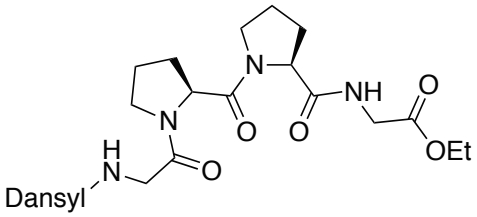

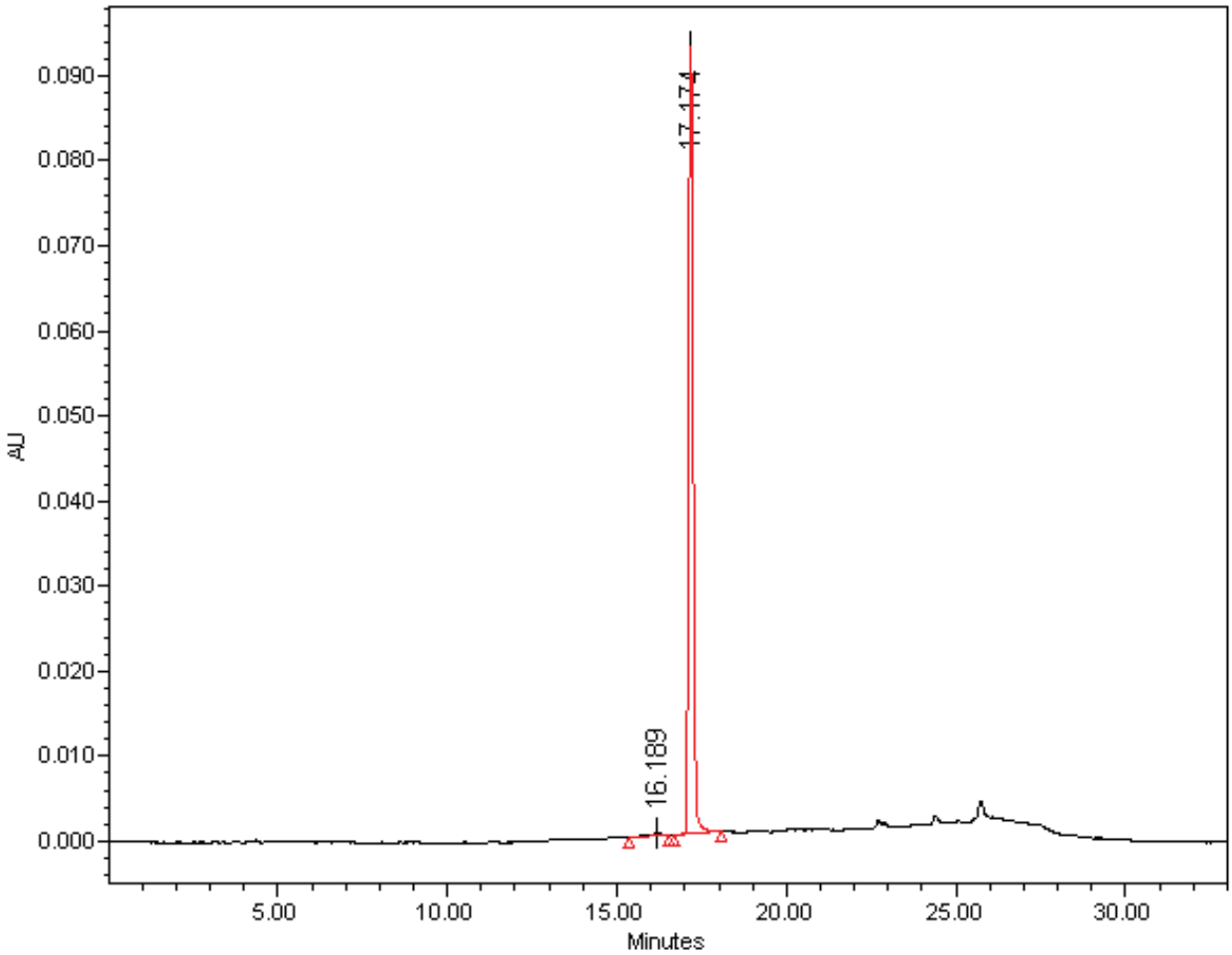

Peak	Retention Time (min)	Area (μV·s)	% Area	Height (μV)
1	16.189	8436	1.00	460
2	**17.174**	**837020**	**99.00**	**92761**

II. NMR Spectra

^{1}H NMR ($CDCl_3$) and ^{13}C NMR ($CDCl_3$) of 3-methoxycarbonylpyridine *N*-oxide

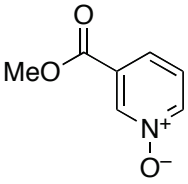

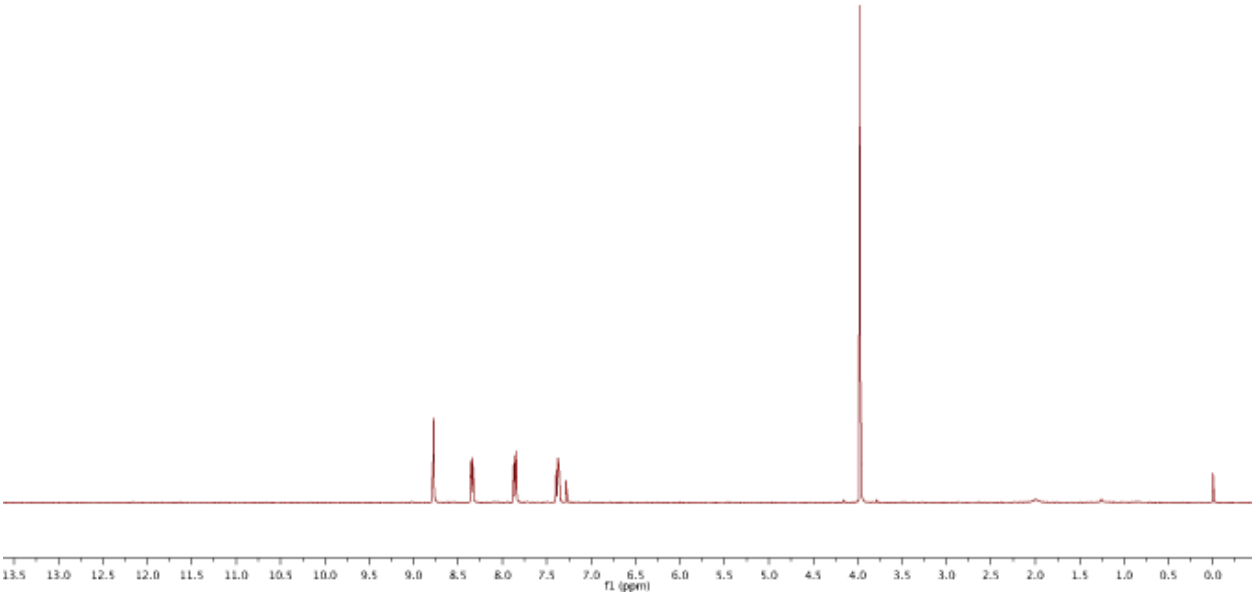

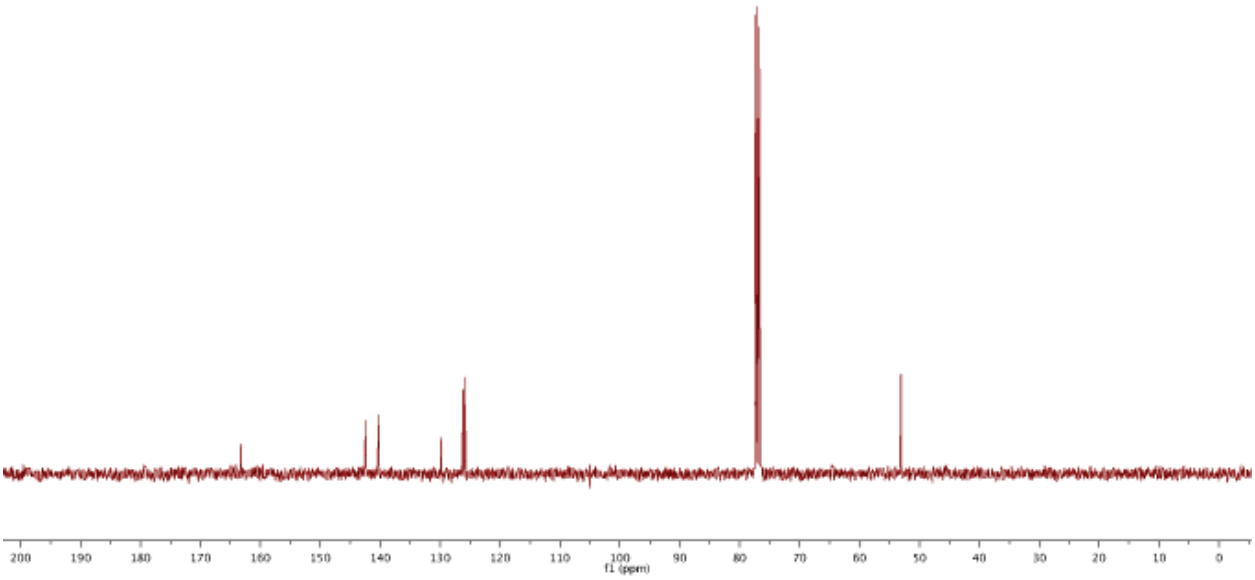

^{1}H NMR ($CDCl_3$) and ^{13}C NMR ($CDCl_3$) of 4-methoxycarbonylpyridine *N*-oxide

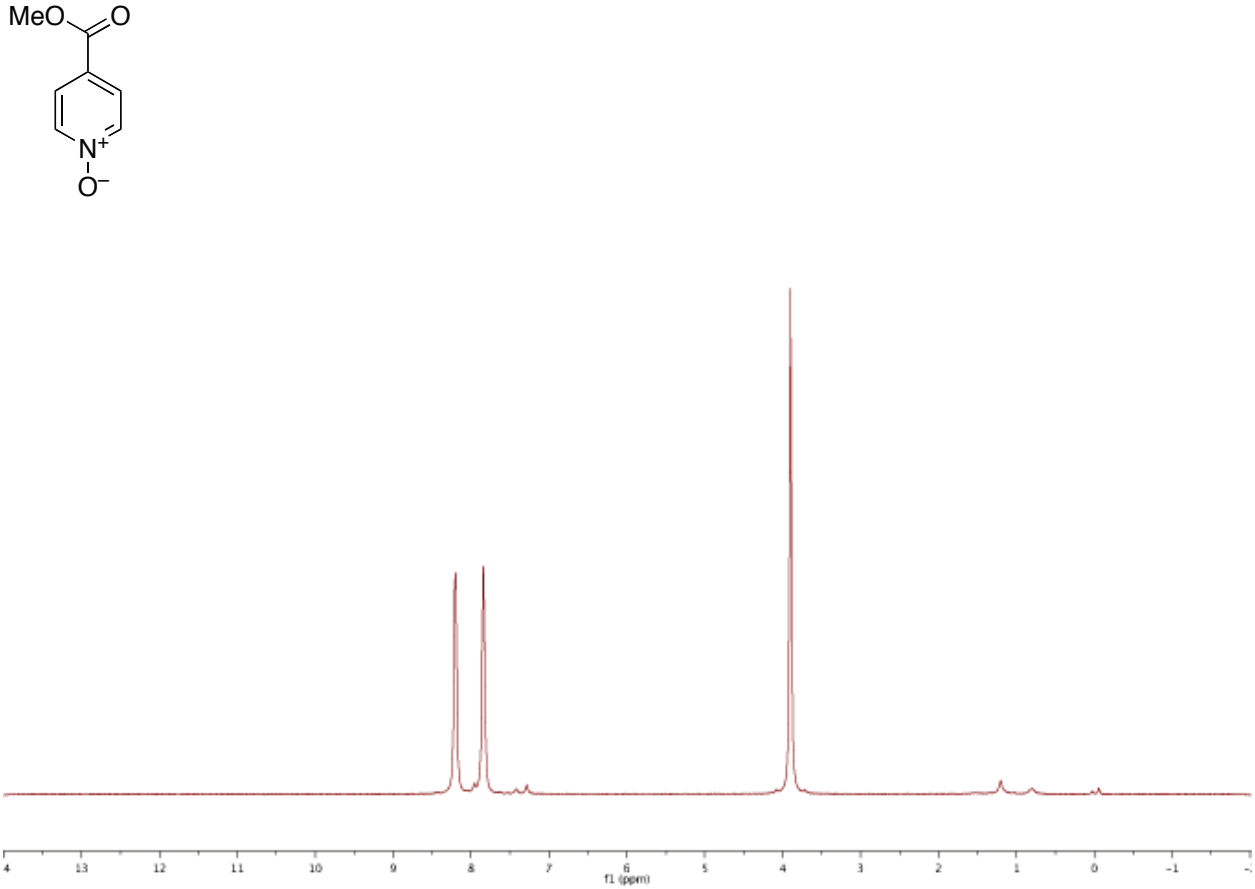

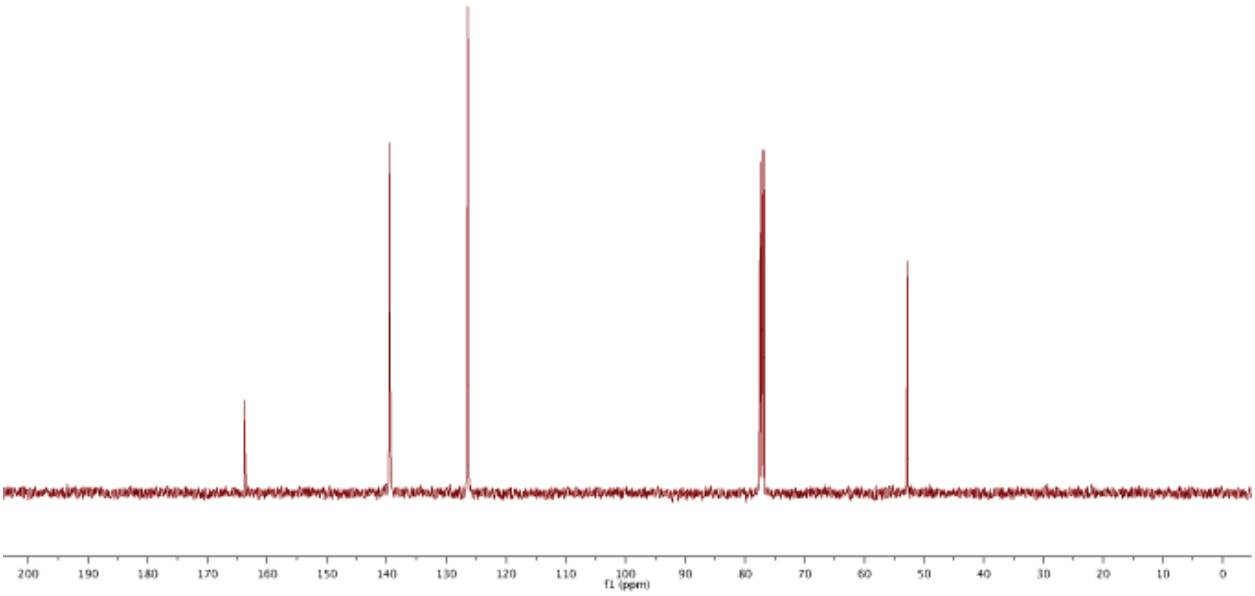

^{1}H NMR ($CDCl_3$) and ^{13}C NMR ($CDCl_3$) of
5-methoxycarbonyl-2-(4-methoxycarbonylpyridin-2-yl)pyridine *N*-oxide

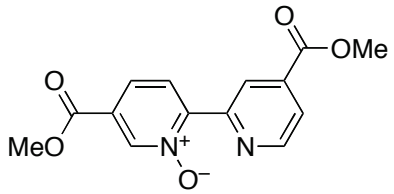

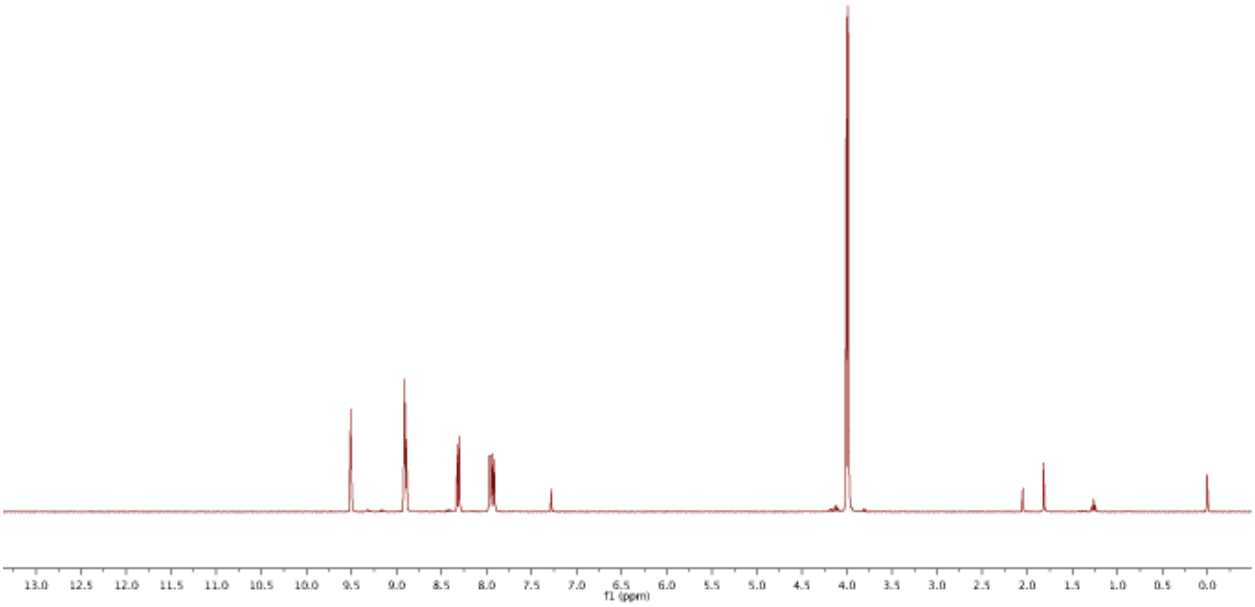

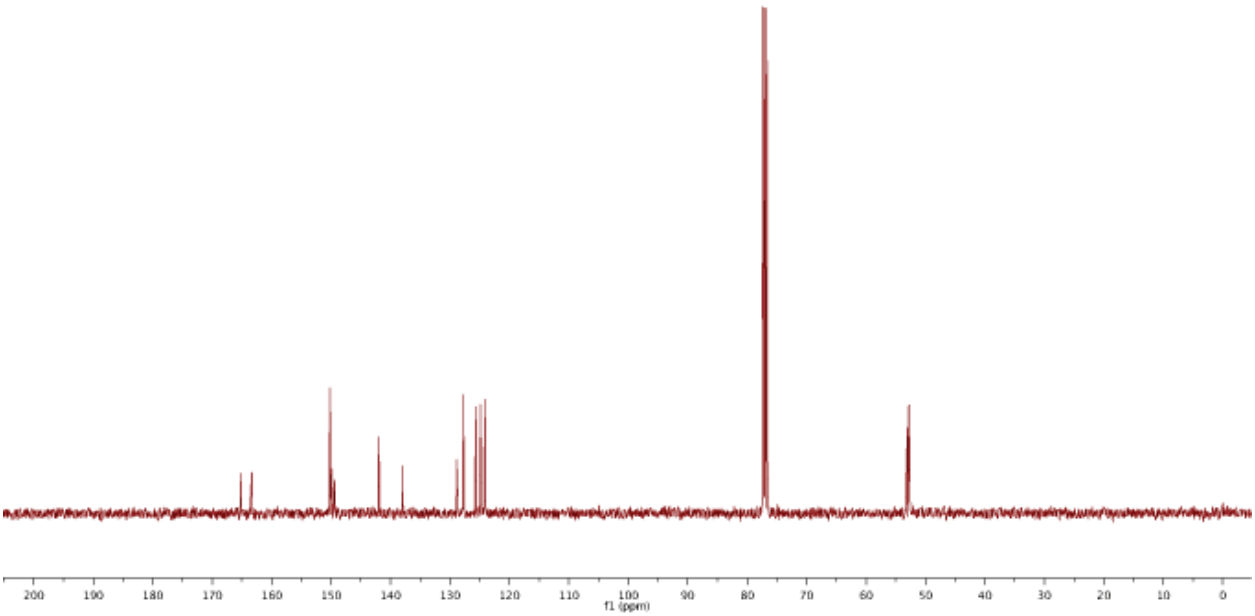

^{1}H NMR ($CDCl_3$) and ^{13}C NMR ($CDCl_3$) of 4-methoxycarbonyl-2-(6-methoxycarbonylpyridin-2-yl)pyridine *N*-oxide

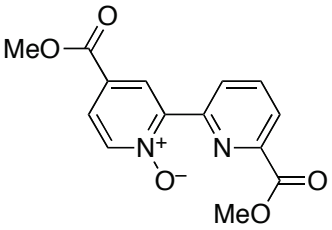

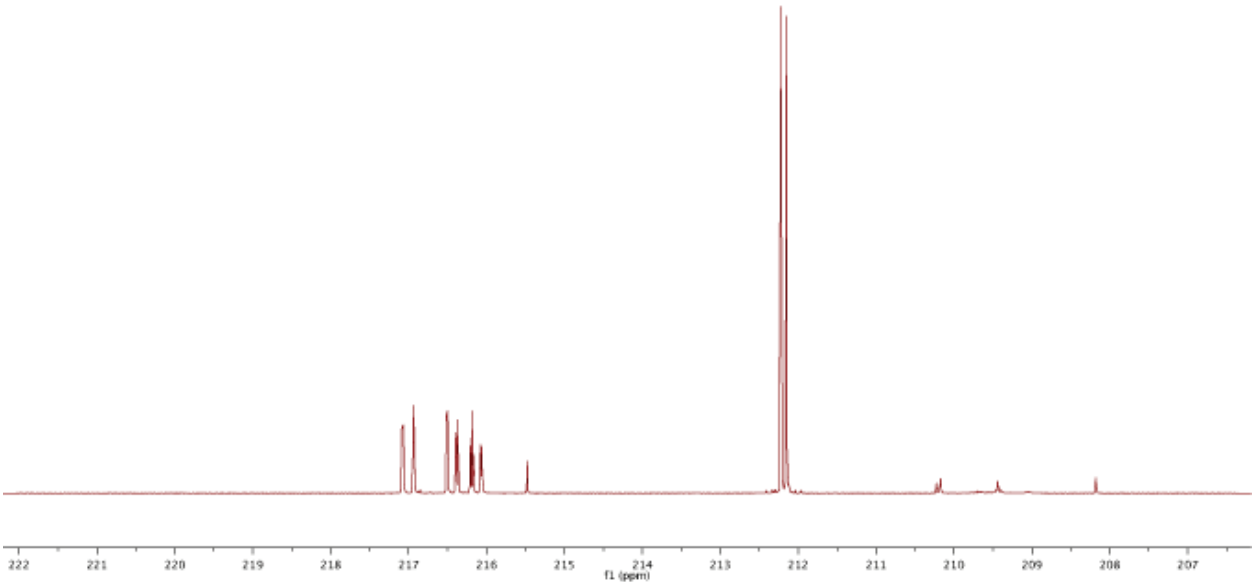

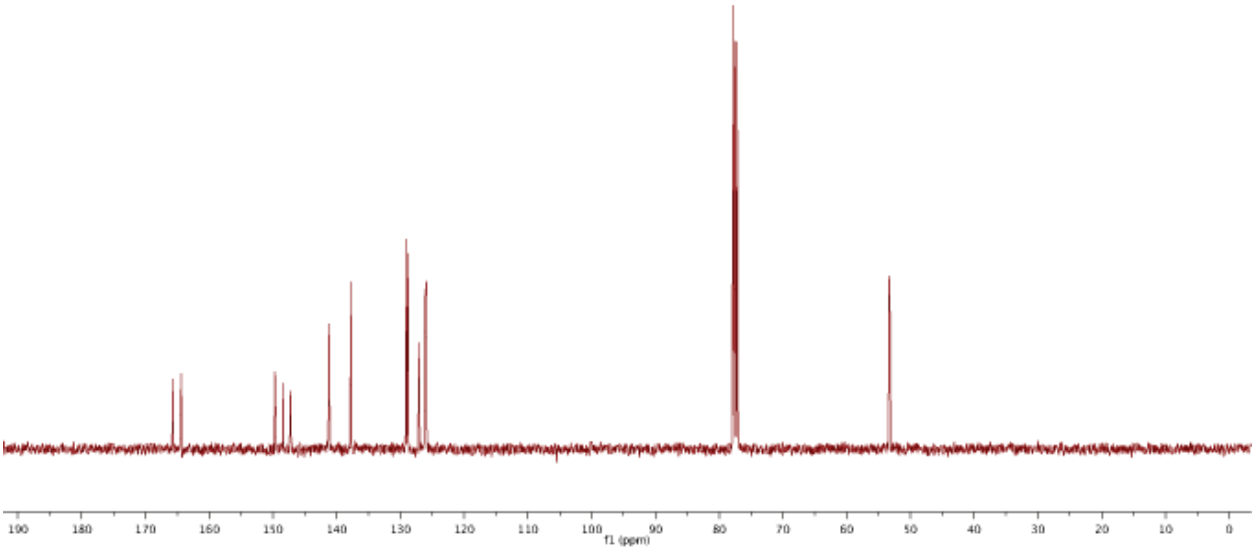

^{1}H NMR ($CDCl_3$) and ^{13}C NMR ($CDCl_3$) of
5-methoxycarbonyl-2-(6-methoxycarbonylpyridin-2-yl)pyridine *N*-oxide

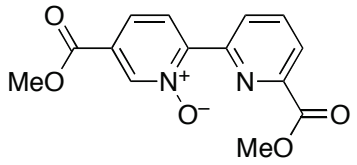

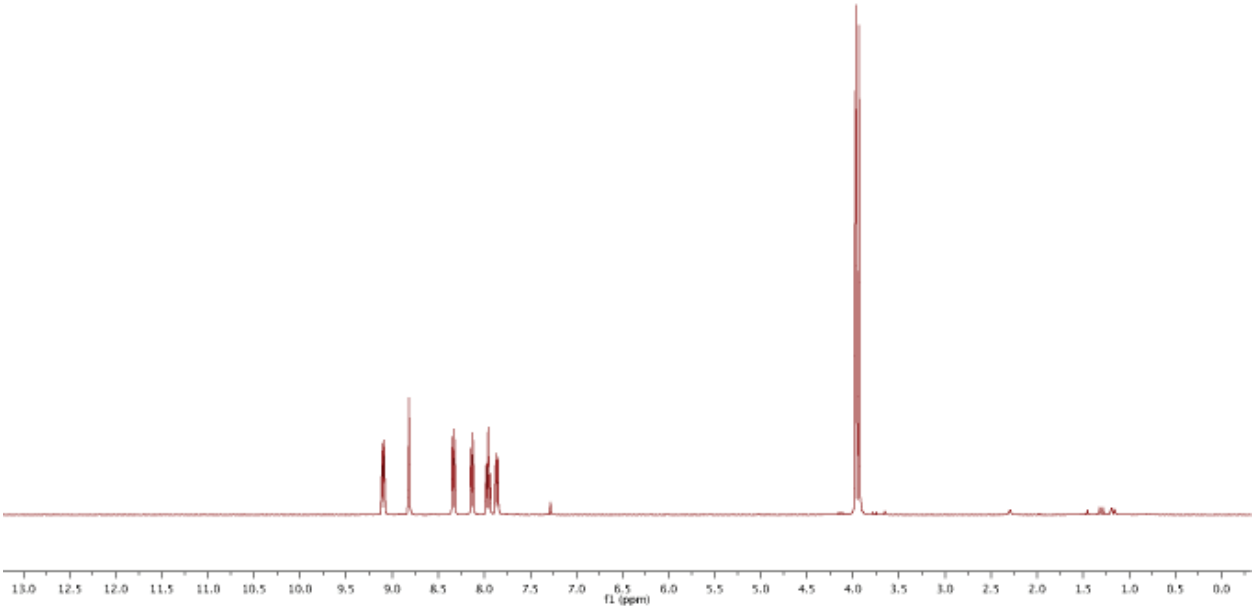

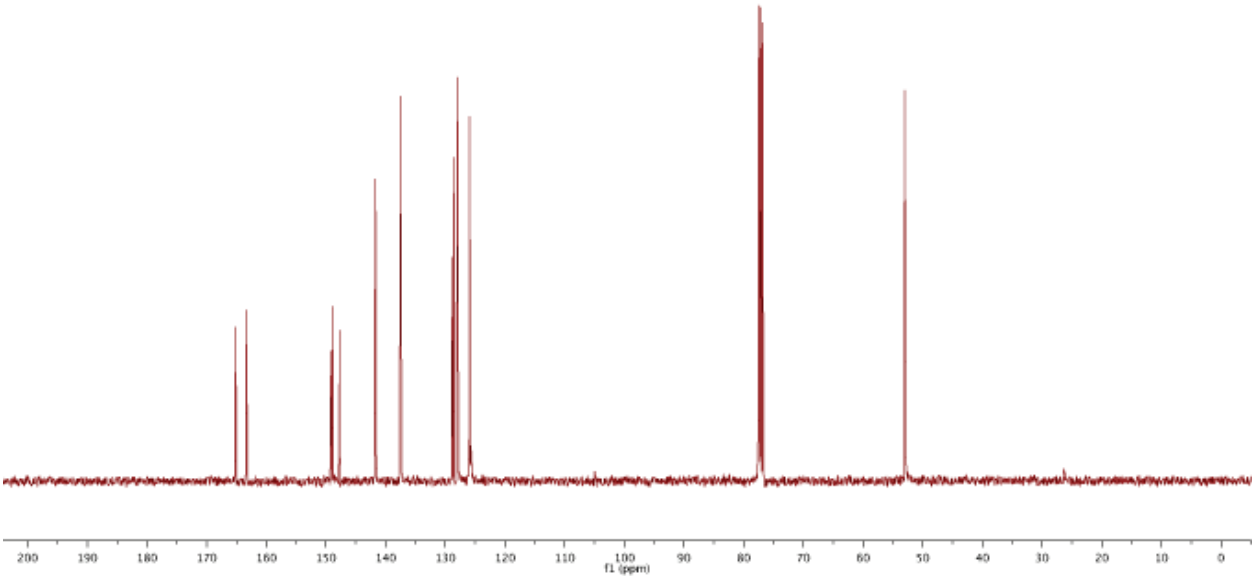

^{1}H NMR ($CDCl_3$) and ^{13}C NMR ($CDCl_3$) of dimethyl 2,2′-bipyridine-4,5′-dicarboxylate

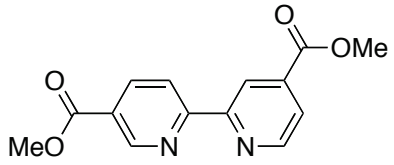

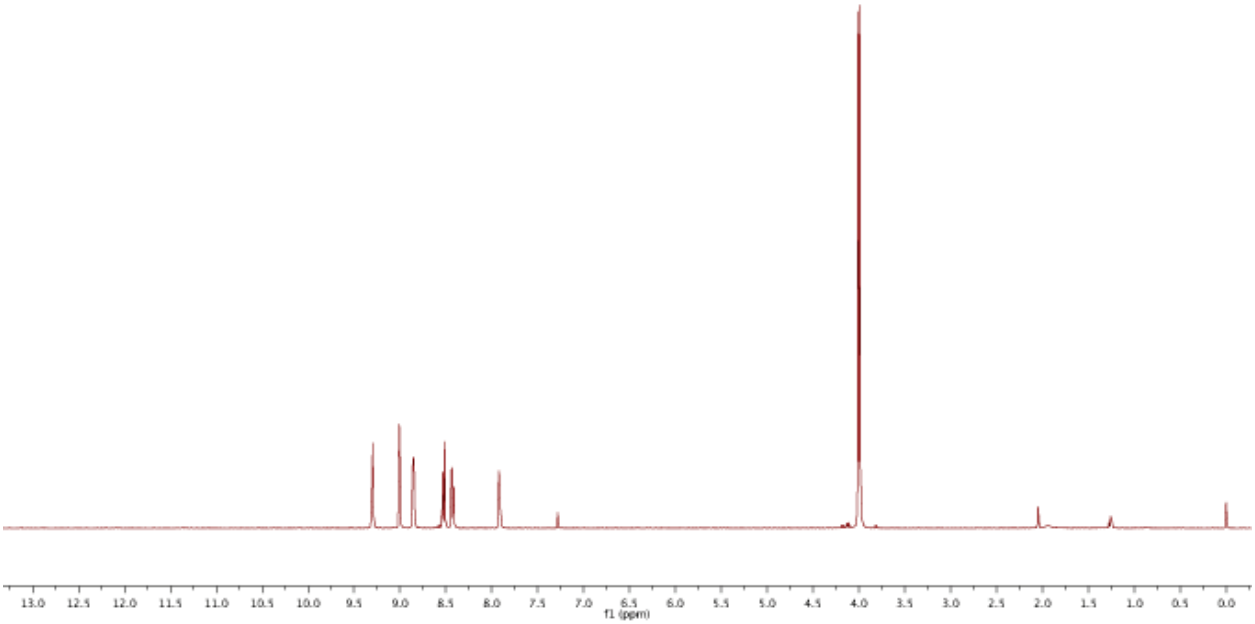

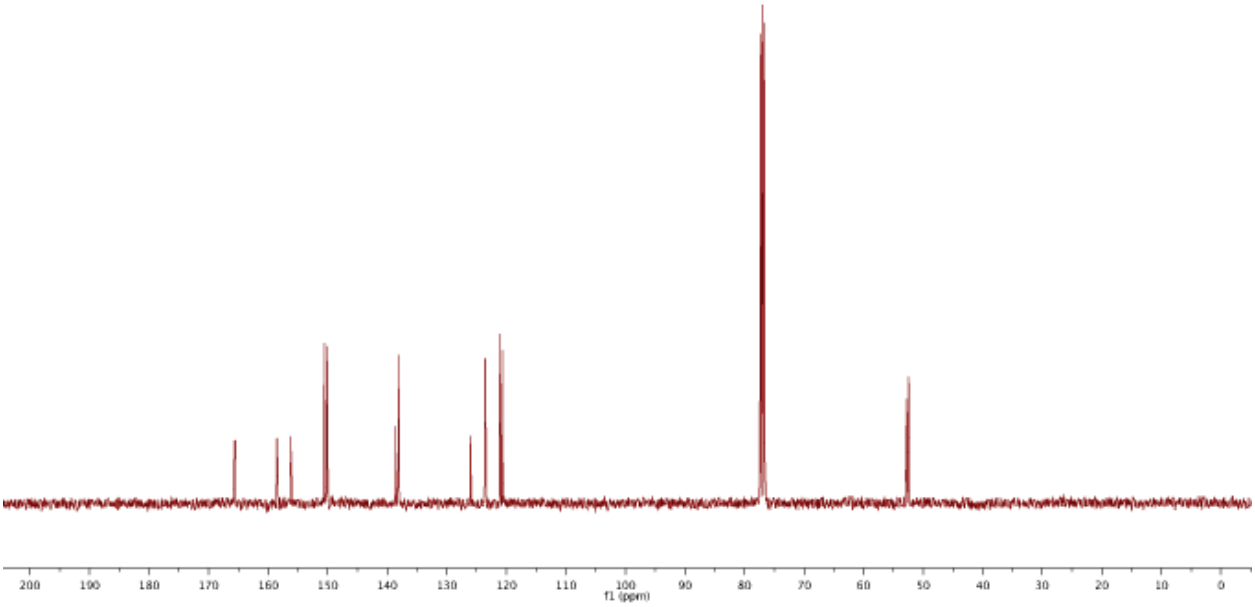

^{1}H NMR ($CDCl_3$) and ^{13}C NMR ($CDCl_3$) of dimethyl 2,2′-bipyridine-4,6′-dicarboxylate

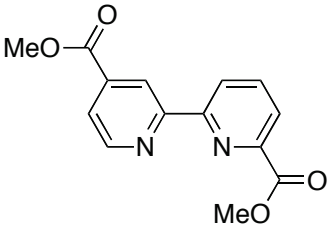

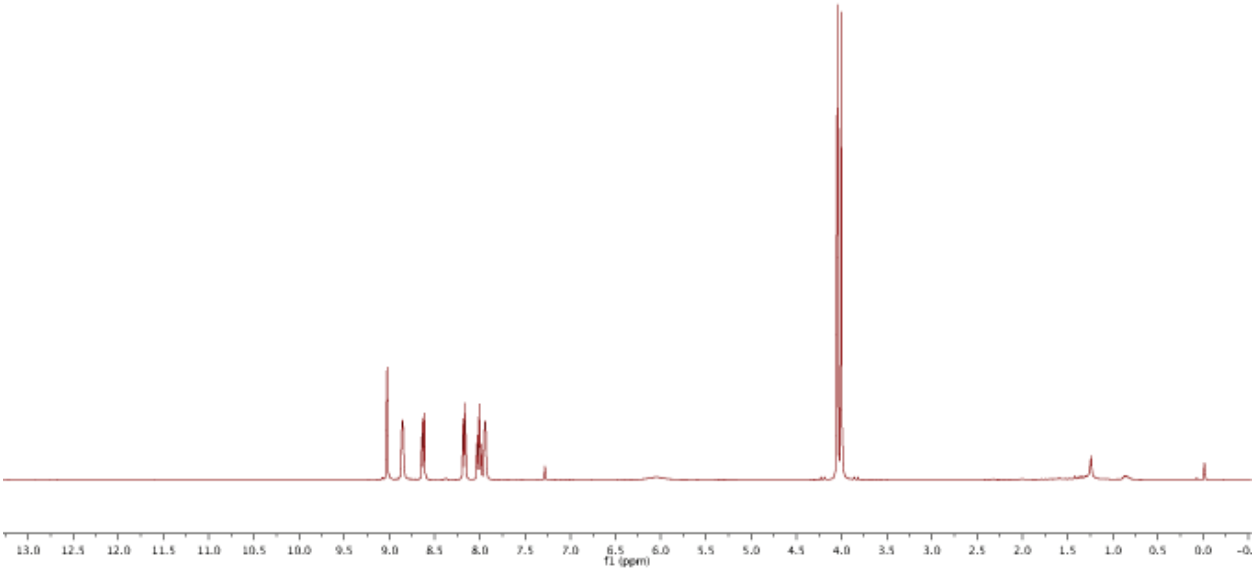

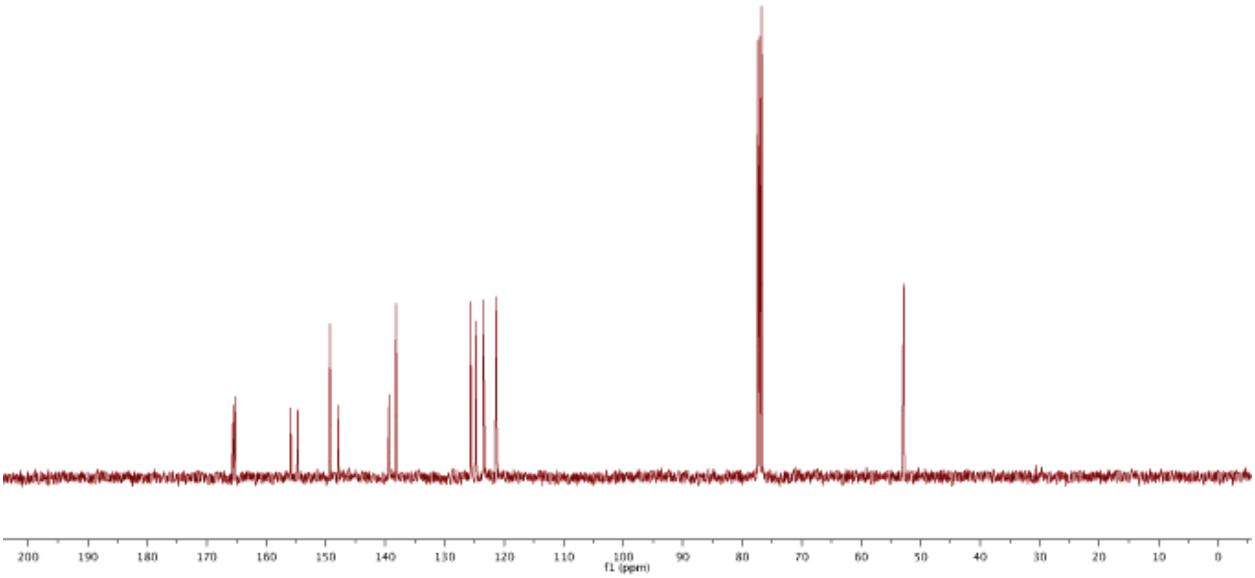

^{1}H NMR ($CDCl_3$) and ^{13}C NMR ($CDCl_3$) of dimethyl 2,2′-bipyridine-5,6′-dicarboxylate

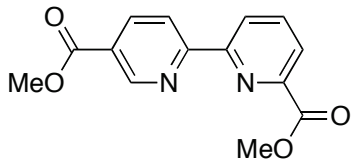

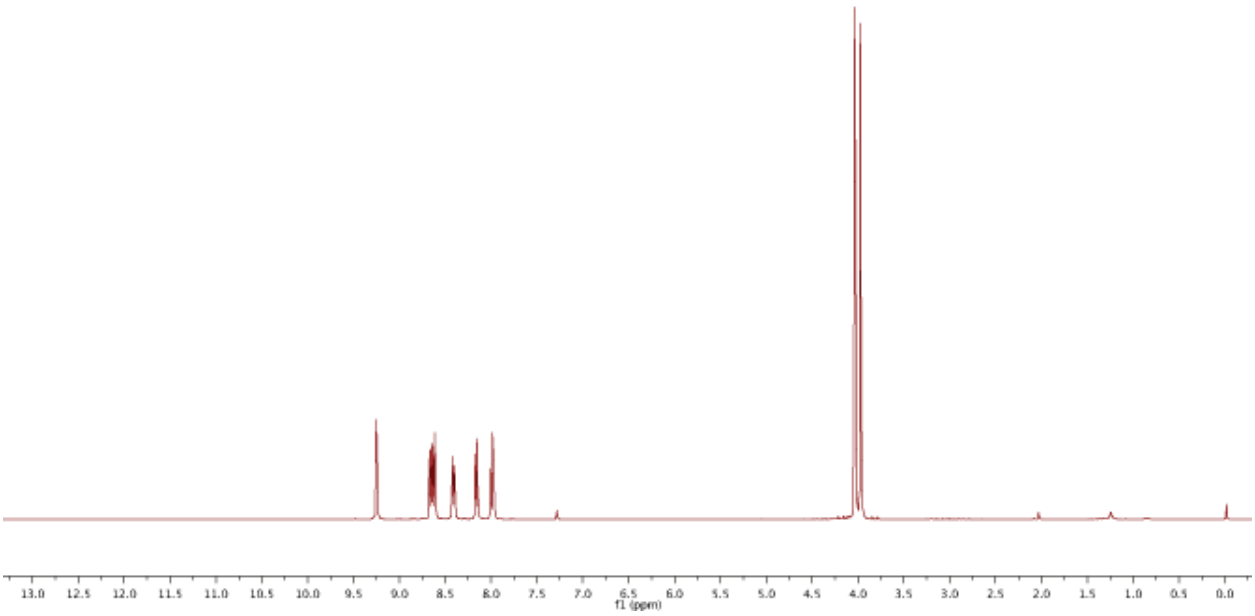

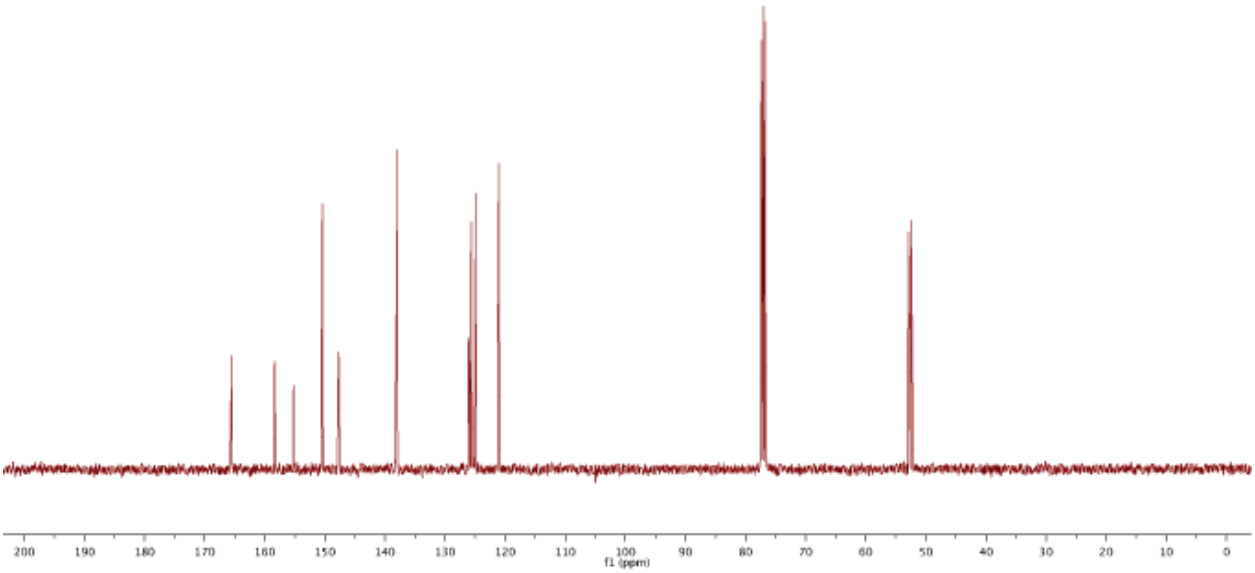

^{1}H NMR (DMSO-d_6) and ^{13}C NMR (DMSO-d_6) of 2,2′-bipyridine-4,5′-dicarboxylic acid (4c)

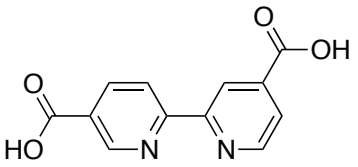

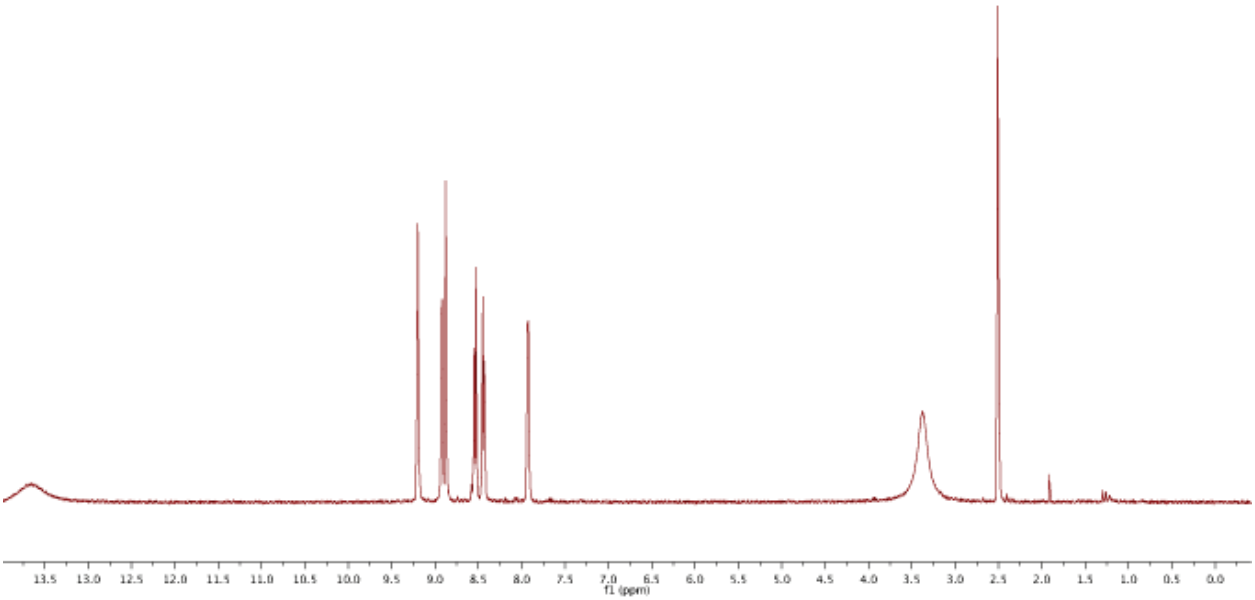

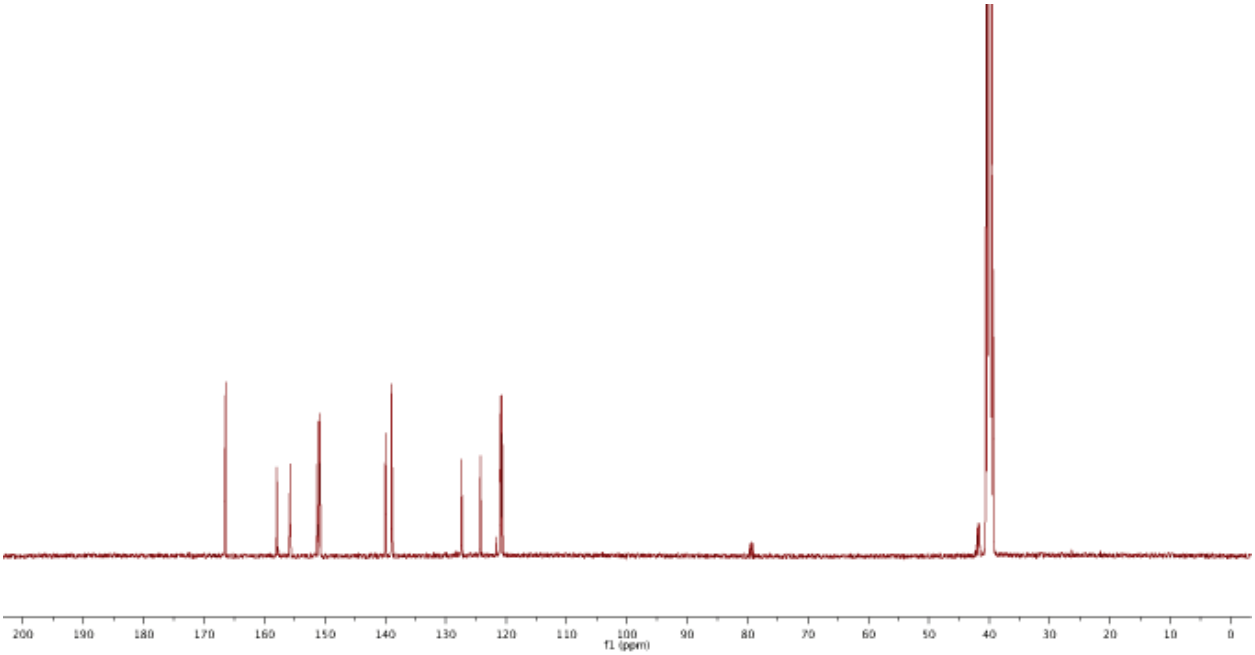

^{1}H NMR (DMSO-d_6) and ^{13}C NMR (DMSO-d_6) of 2,2′-bipyridine-4,6′-dicarboxylic acid (4d)

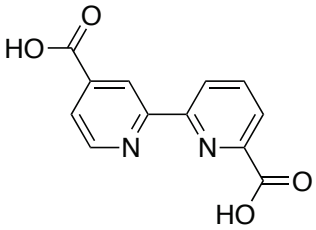

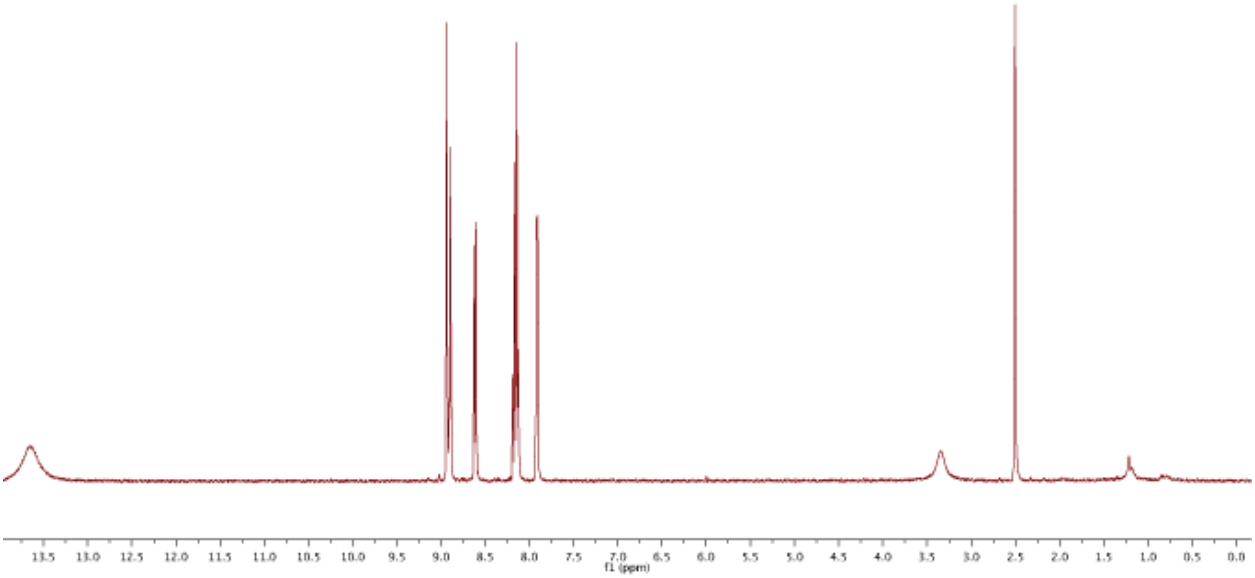

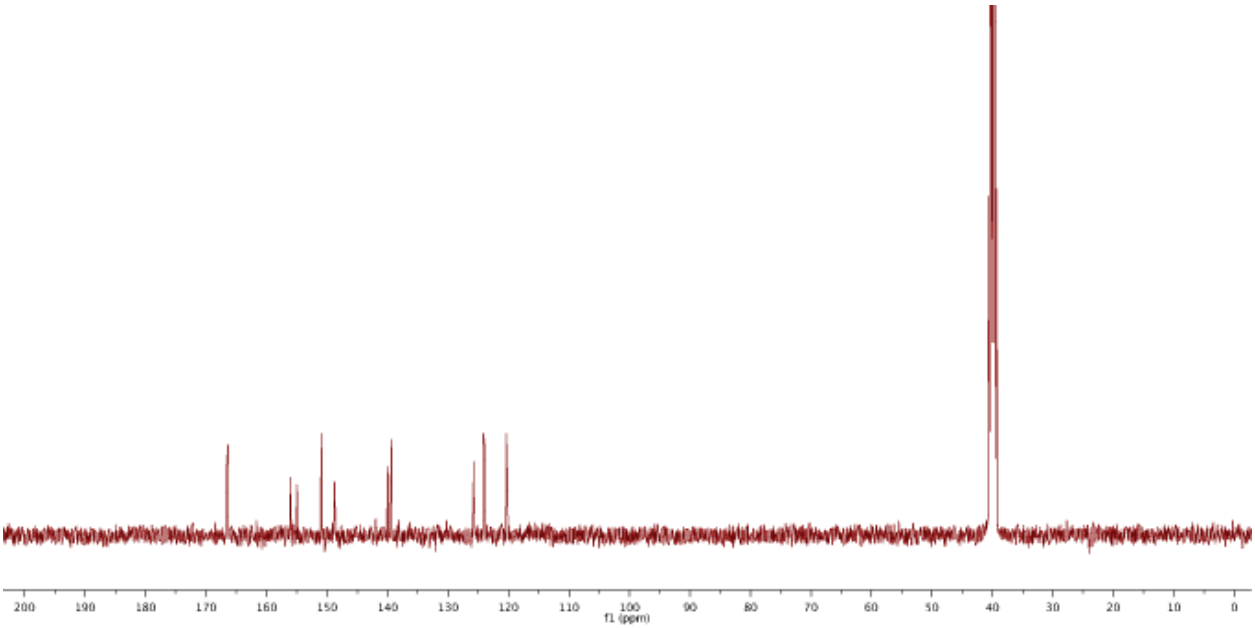

^{1}H NMR (DMSO-d_6) and ^{13}C NMR (DMSO-d_6) of 2,2′-bipyridine-5,6′-dicarboxylic acid (4f)

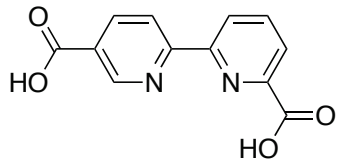

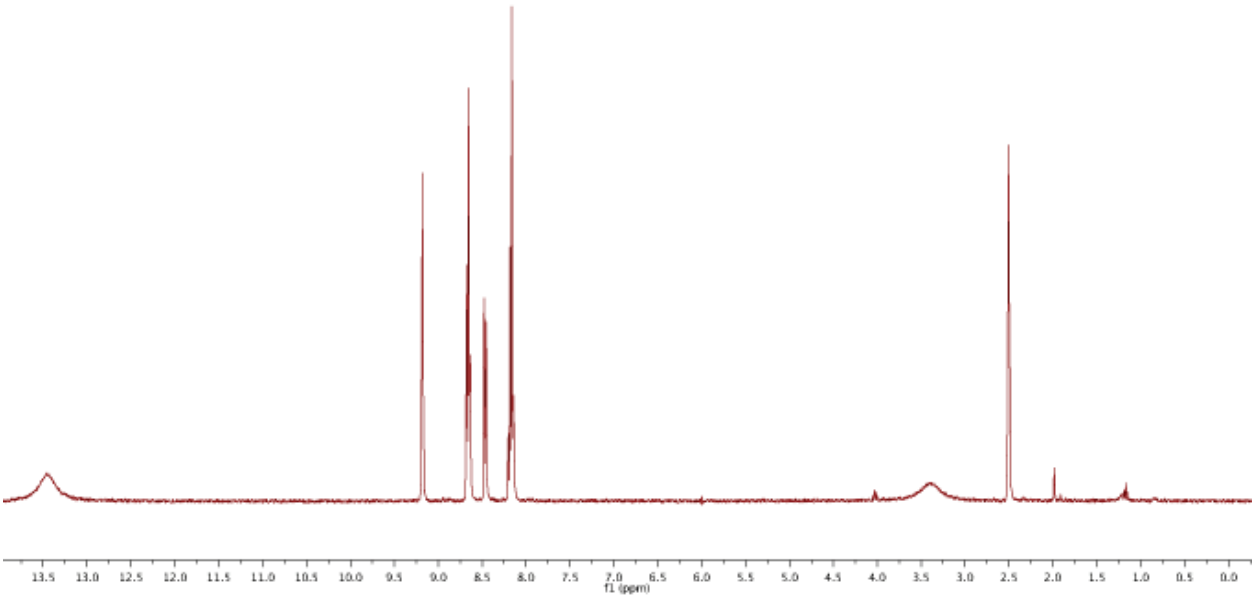

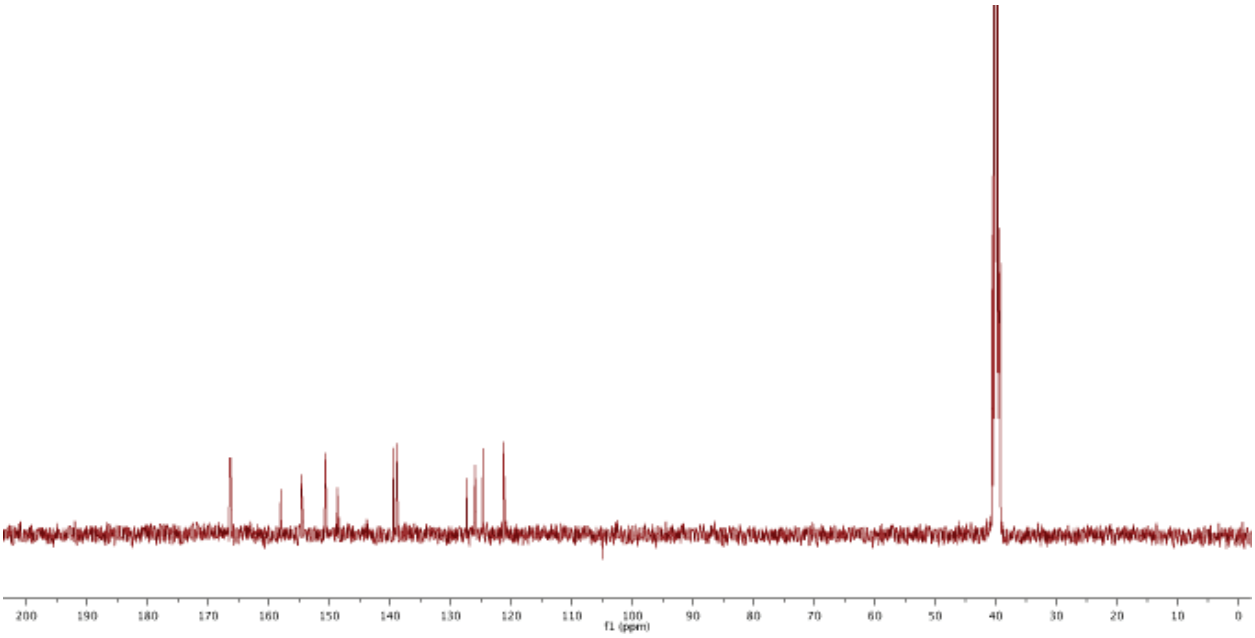

^{1}H NMR ($CDCl_3$) and ^{13}C NMR ($CDCl_3$) of *N*-(methoxyoxalyl)glycine ethyl ester

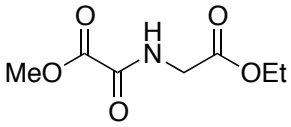

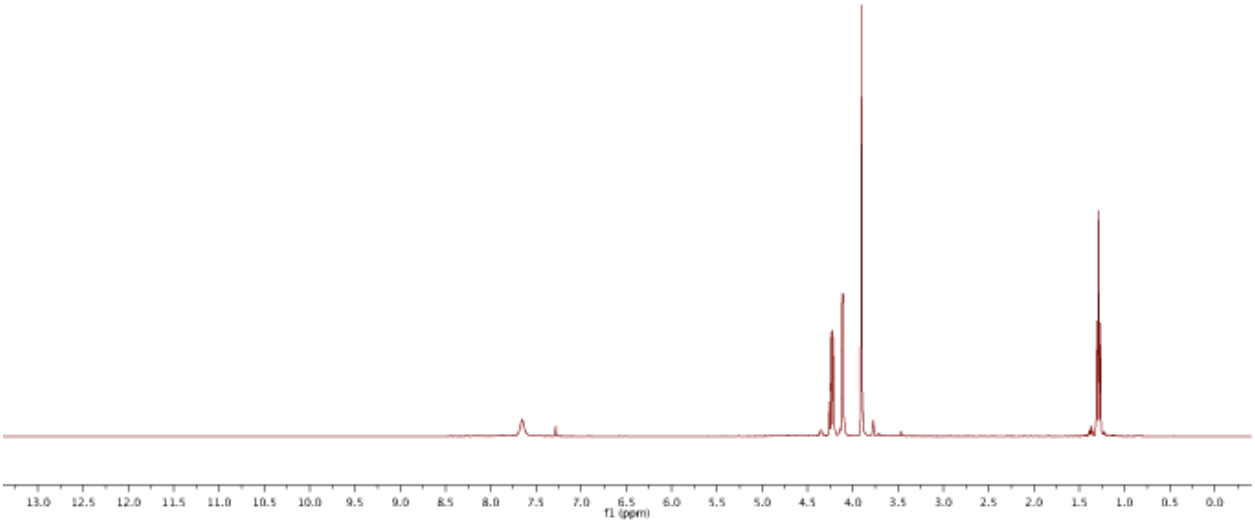

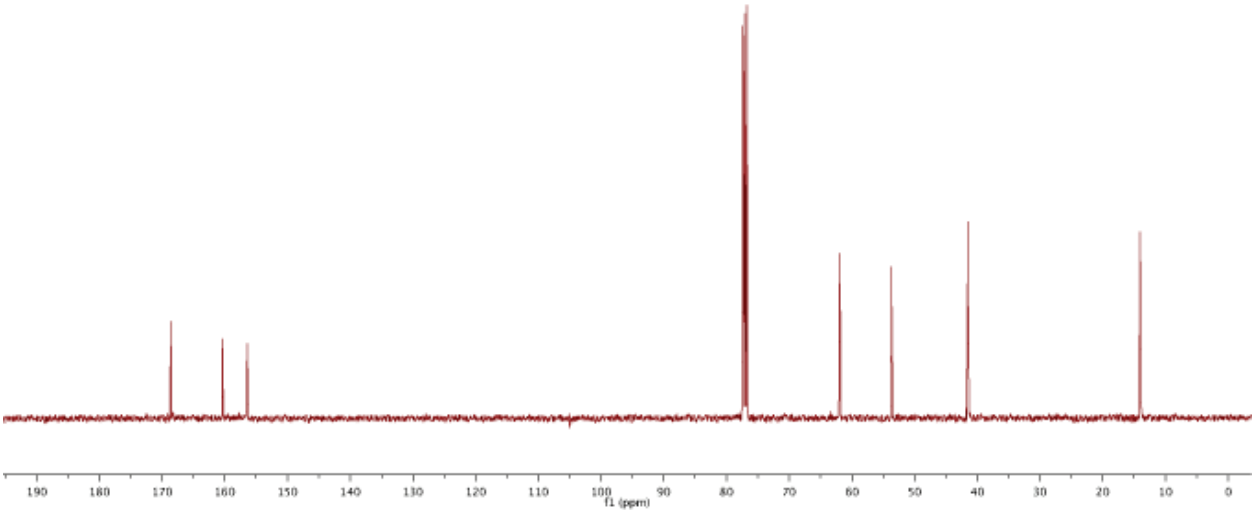

^{1}H NMR (DMSO-d_6) and ^{13}C NMR (DMSO-d_6) of *N*-oxalylglycine (2)

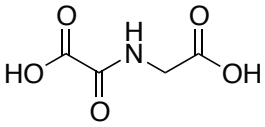

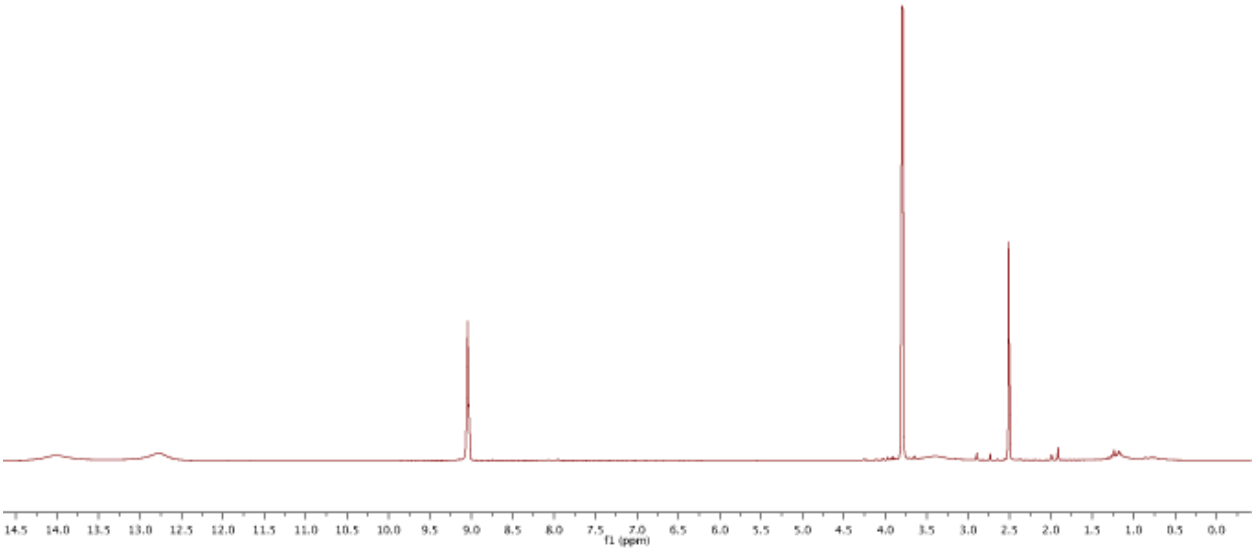

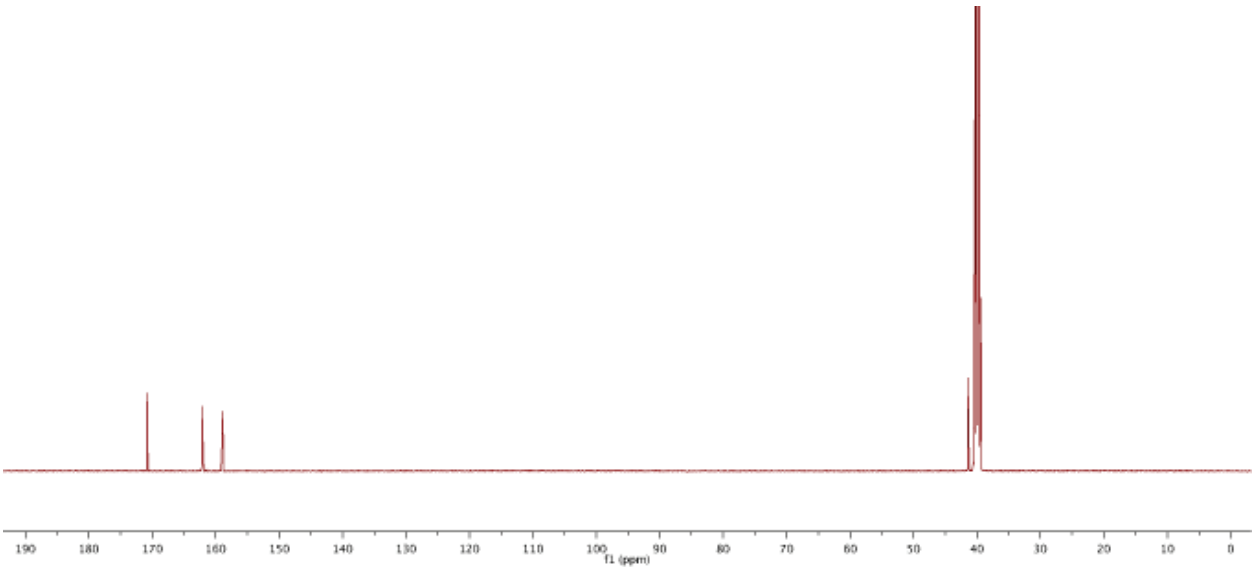

^{1}H NMR ($CDCl_3$) and ^{13}C NMR ($CDCl_3$) of Cbz-Pro-Pro-Gly-OEt

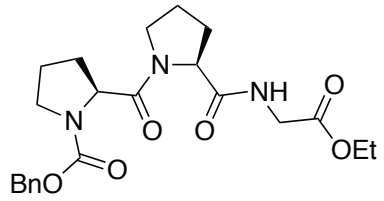

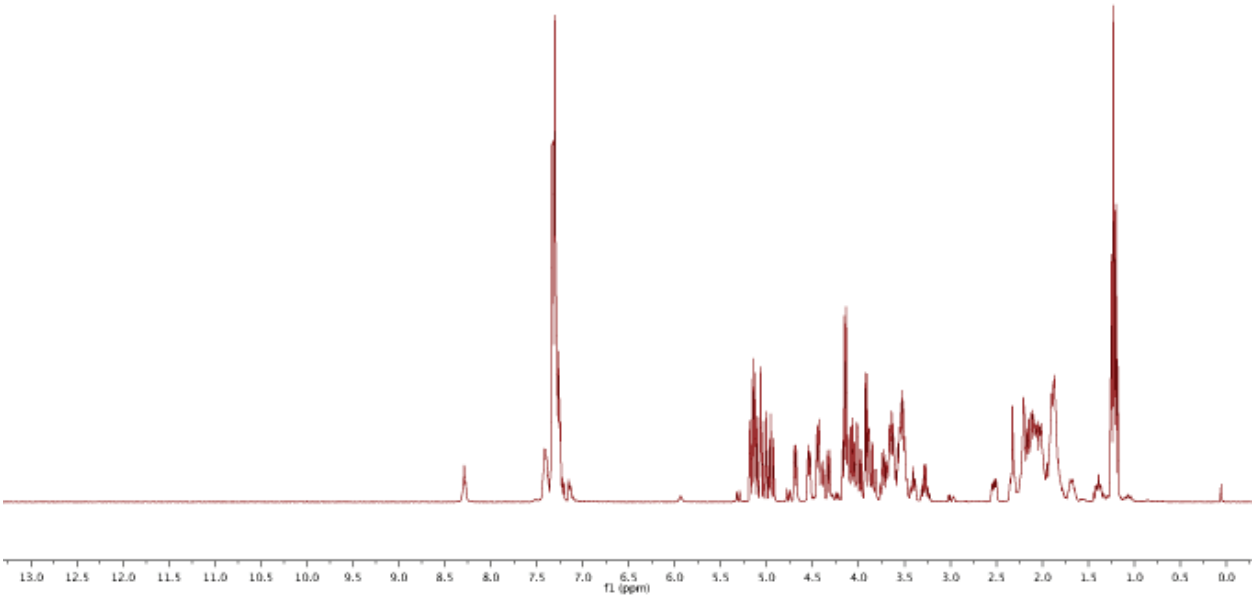

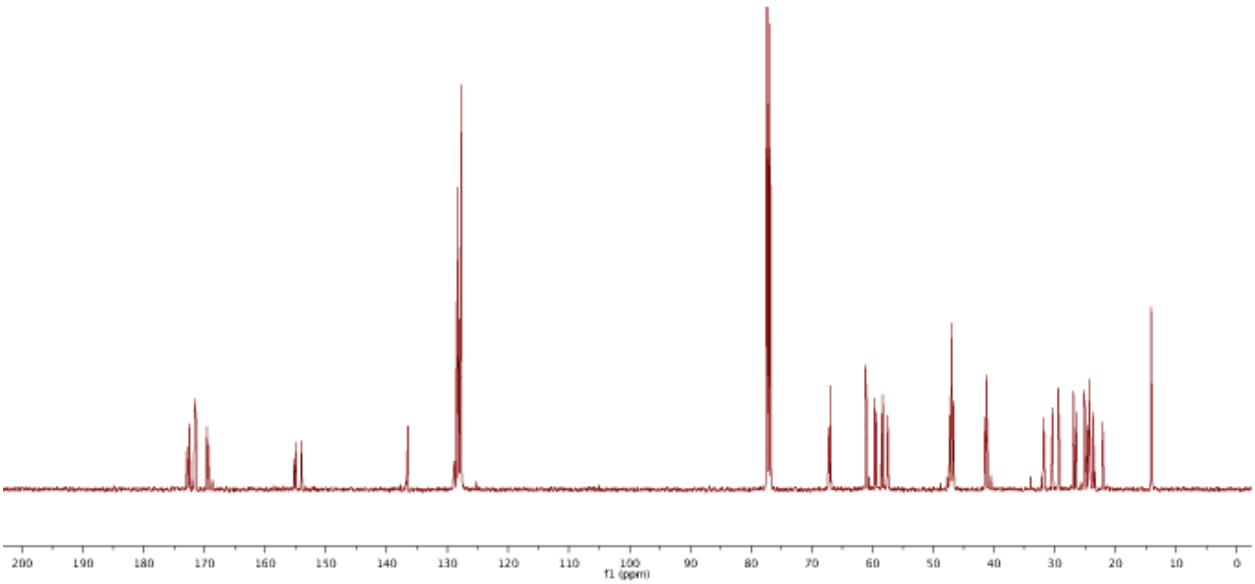

^{1}H NMR ($CDCl_3$) and ^{13}C NMR ($CDCl_3$) of Dansyl-Gly-Pro-Pro-Gly-OEt

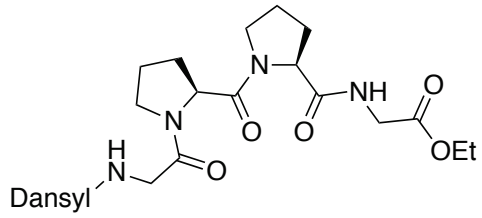

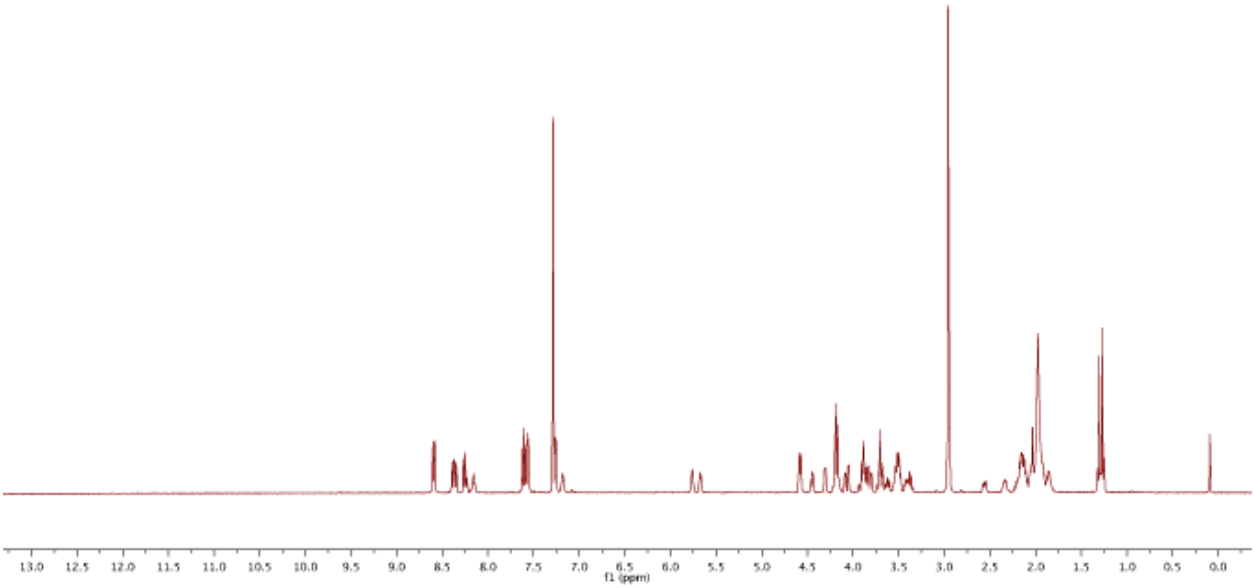

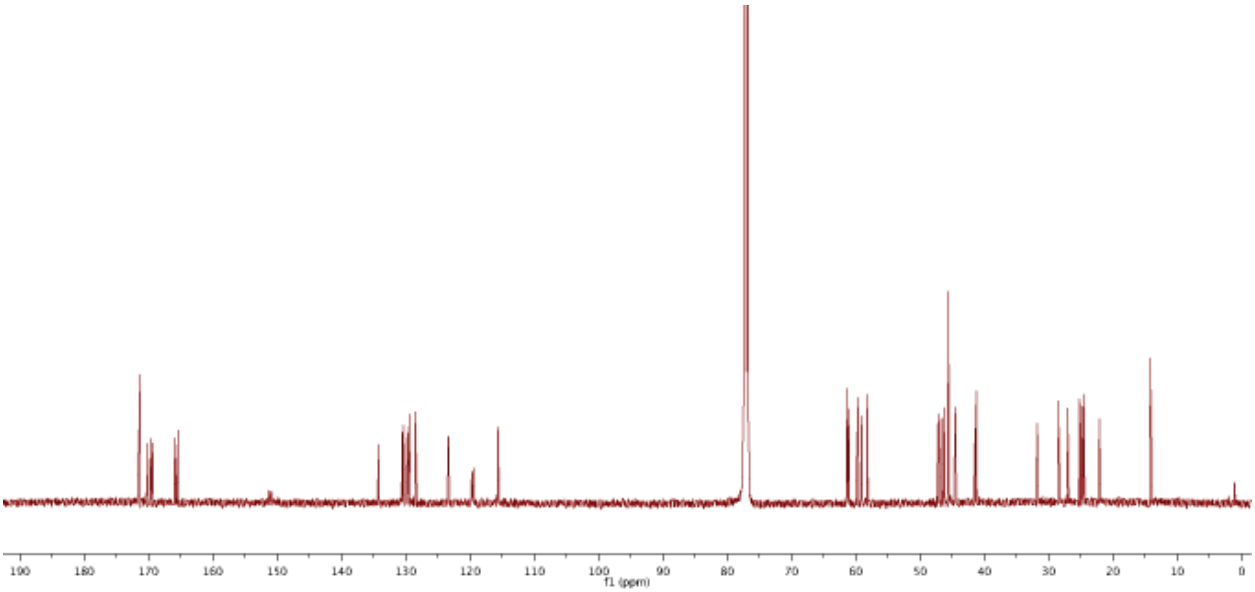

III. Absorption spectra of bipyridine ligands and their complexes with Fe(II)

Compound 1 and Fe(1)$_3$

300 μM **1** ± 100 μM $FeSO_4$ in 10 mM sodium phosphate buffer, pH 7.0

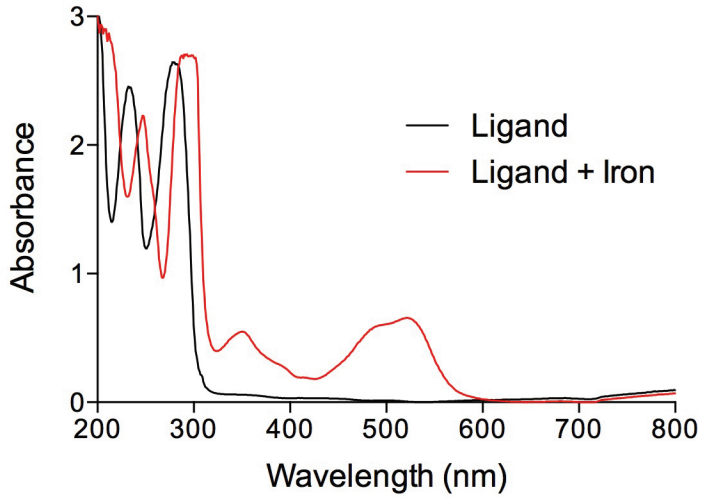

λ_{max} = 523 nm, ε_{523} = (9000 ± 100) $M^{-1}cm^{-1}$

Compound 4b and Fe(4b)$_3$

300 μM **4b** ± 100 μM $FeSO_4$ in 10 mM sodium phosphate buffer, pH 7.0

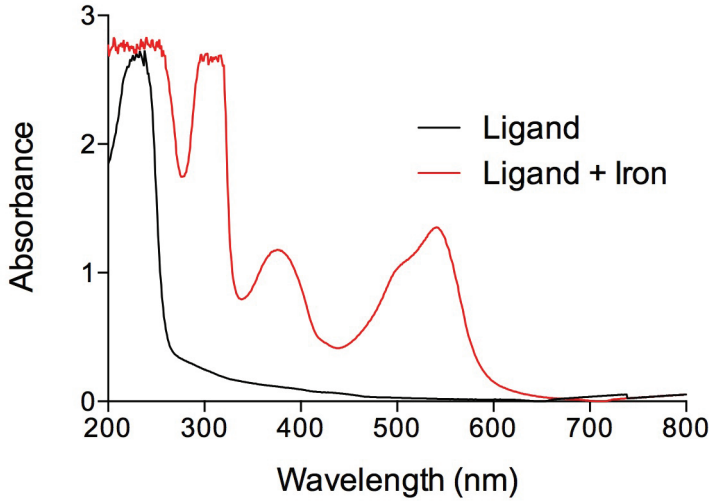

λ_{max} = 541 nm, ε_{541} = (15,090 ± 60) $M^{-1}cm^{-1}$

Compound 4c and Fe(4c)$_3$

300 μM **4c** ± 100 μM $FeSO_4$ in 10 mM sodium phosphate buffer, pH 7.0

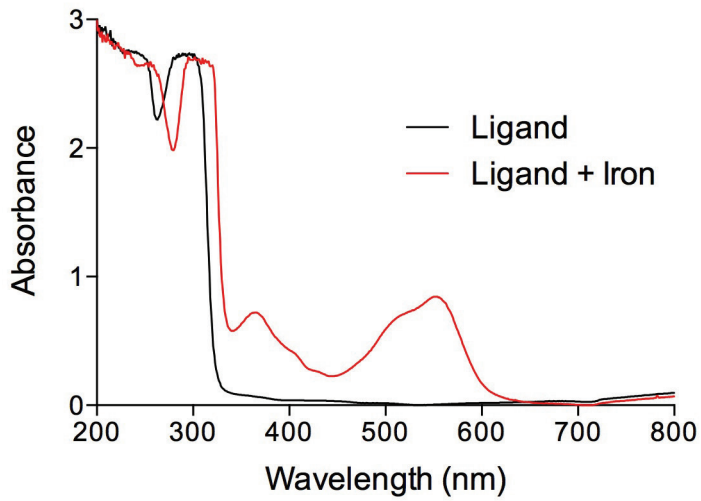

λ_{max} = 553 nm, ε_{553} = (11,200 ± 60) $M^{-1}cm^{-1}$

Compound 4d and Fe(4d)$_2$

200 μM **4d** ± 100 μM $FeSO_4$ in 10 mM sodium phosphate buffer, pH 7.0

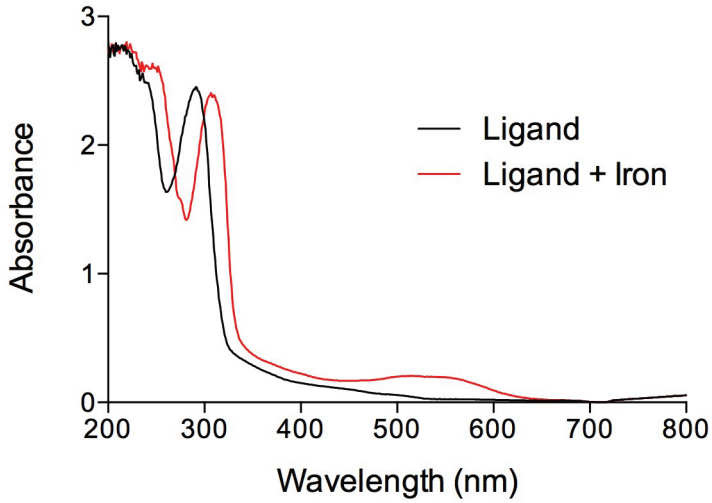

λ_{max} = 559 nm, ε_{559} = (1690 ± 20) $M^{-1}cm^{-`1}$

Compound 4e and Fe(II)·(4e)$_3$

300 μM **4e** ± 100 μM $FeSO_4$ in 10 mM sodium phosphate buffer, pH 7.0

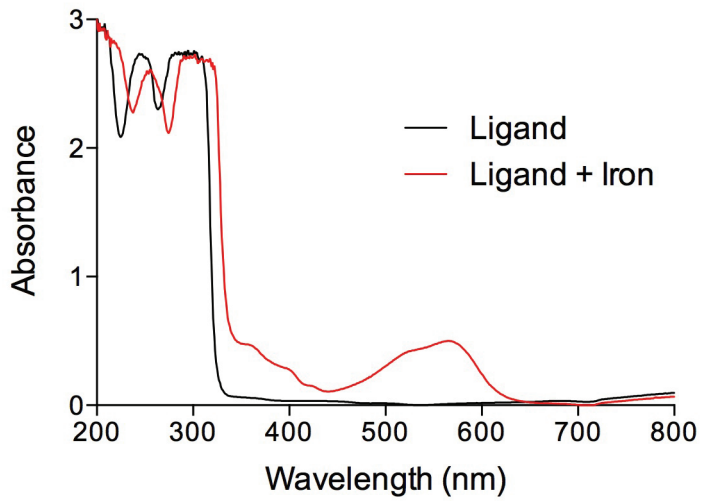

λ_{max} = 566 nm, ε_{566} = (7500 ± 100) $M^{-1}cm^{-1}$

Compound 4f and Fe(II)·(4f)$_2$

200 μM **4f** ± 100 μM $FeSO_4$ in 10 mM sodium phosphate buffer, pH 7.0

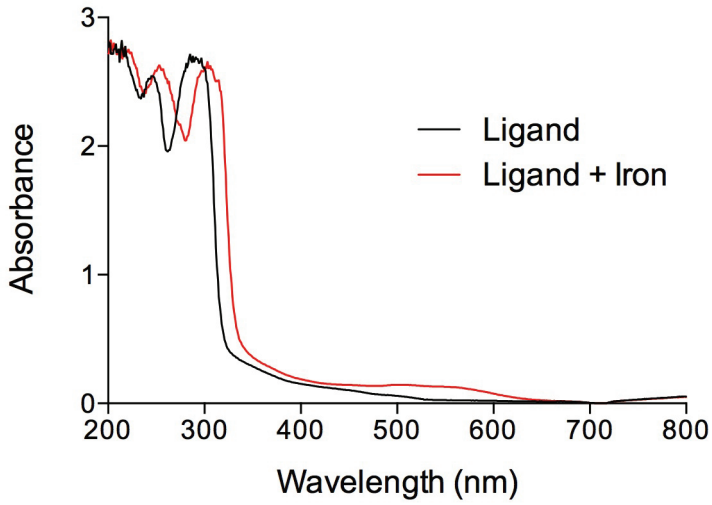

λ_{max} = 566 nm, ε_{566} = (1220 ± 30) $M^{-1}cm^{-1}$

Compound 3a

300 μM **3a** ± 100 μM $FeSO_4$ in 10 mM sodium phosphate buffer, pH 7.0

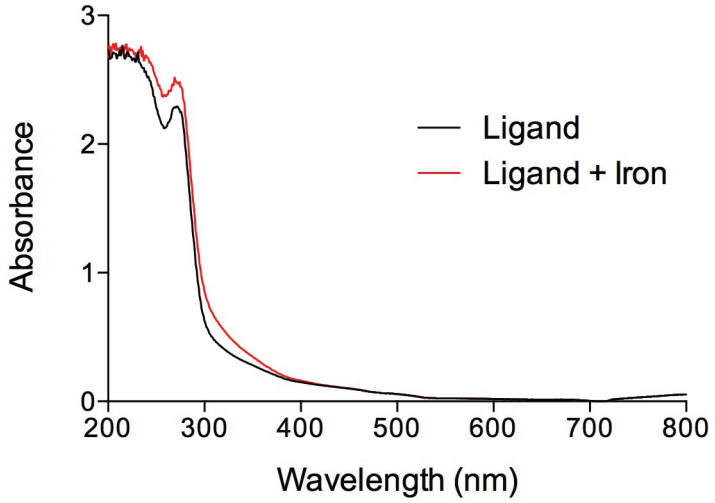

Compound 4g

300 μM **4g** ± 100 μM $FeSO_4$ in 10 mM sodium phosphate buffer, pH 7.0

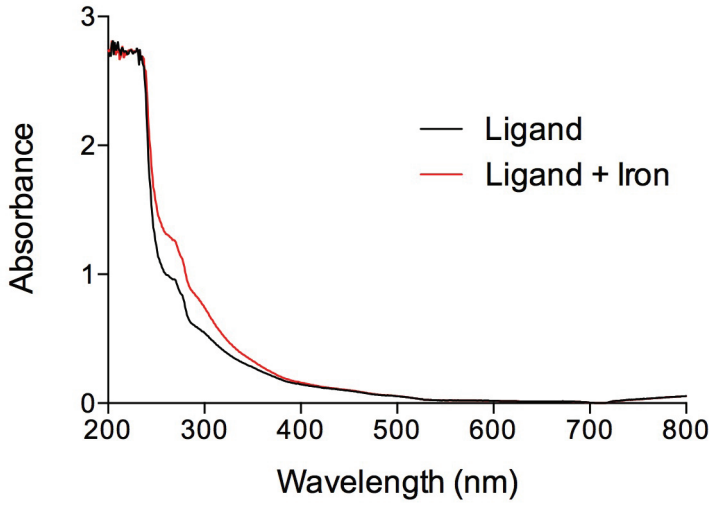

IV. Plots of Fe(II) binding by bipyridine ligands

Fe·(1)$_3^{2+}$

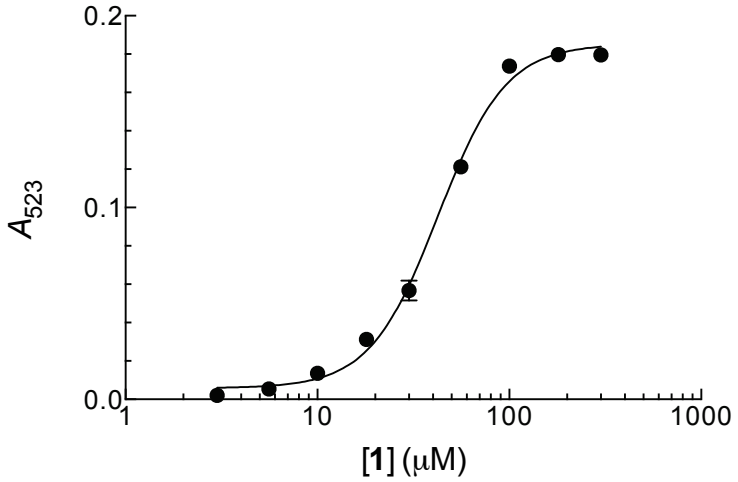

Fe_{20}-EC_{50} = (43 ± 2) μM, slope = 2.5 ± 0.3
top = 0.185 ± 0.005, bottom = 0.006 ± 0.004, R^2 = 0.997

Fe(II)·(4b)$_3$

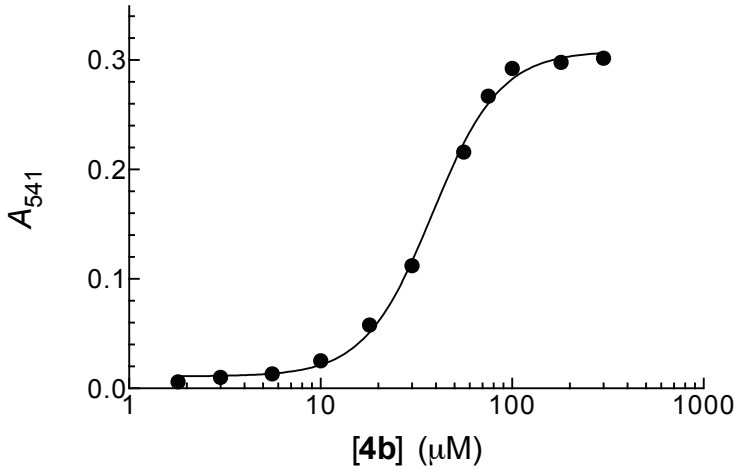

Fe_{20}-EC_{50} = (38 ± 1) μM, slope = 2.5 ± 0.2
top = 0.308 ± 0.006, bottom = 0.011 ± 0.004, R^2 = 0.998

Fe(II)·(4c)$_3$

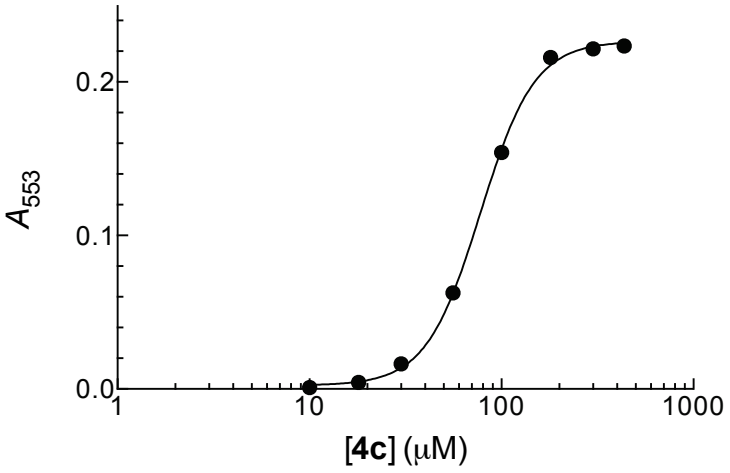

Fe_{20}-EC_{50} = (78 ± 2) μM, slope = 3.1 ± 0.2
top = 0.227 ± 0.003, bottom = 0.002 ± 0.003, R^2 = 0.999

Fe(II)·(4d)$_2$

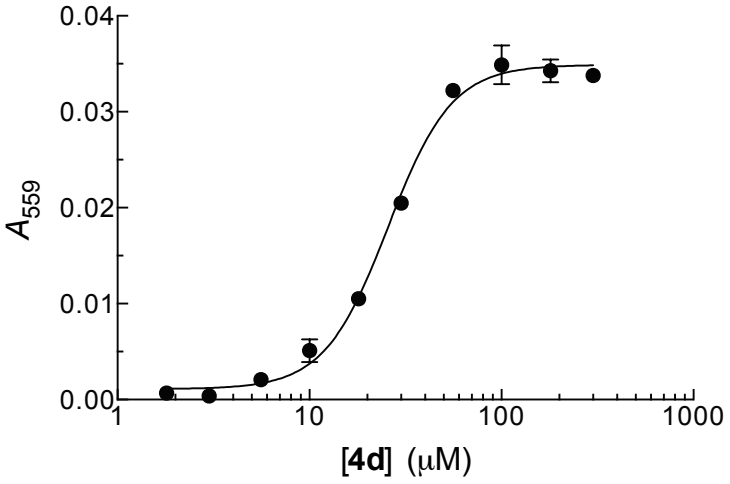

Fe_{20}-EC_{50} = (26 ± 1) μM, slope = 2.6 ± 0.3
top = 0.0349 ± 0.0007, bottom = 0.0011 ± 0.0007, R^2 = 0.997

Fe(II)·(4e)$_3$

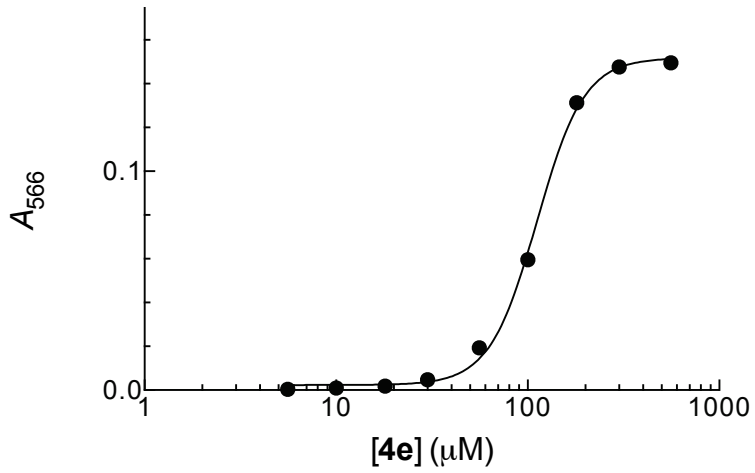

Fe_{20}-EC_{50} = (112 ± 3) μM, slope = 3.5 ± 0.3,
top = 0.152 ± 0.003, bottom = 0.002 ± 0.002, R^2 = 0.998

Fe(II)·(4f)$_2$

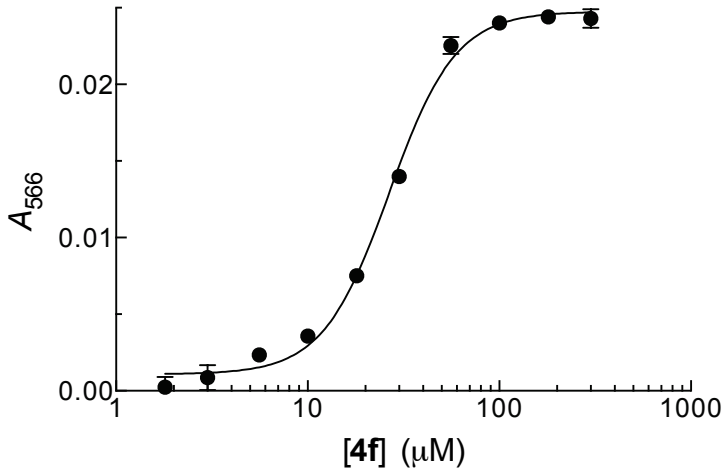

Fe_{20}-EC_{50} = (27 ± 1) μM, slope = 2.5 ± 0.3,
top = 0.0248 ± 0.0005, bottom = 0.0011 ± 0.0005, R^2 = 0.997

V. Job plots of Fe(II) binding by bipyridine ligands

Fe(II)·(1)$_3$

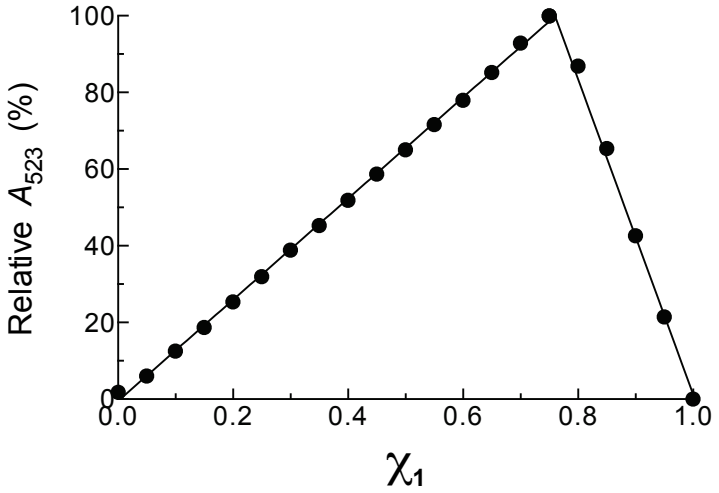

χ_1 at point of intersection = 0.76 ± 0.03, suggesting 3:1 (**1**:Fe) stoichiometry

Fe(II)·(4b)$_3$

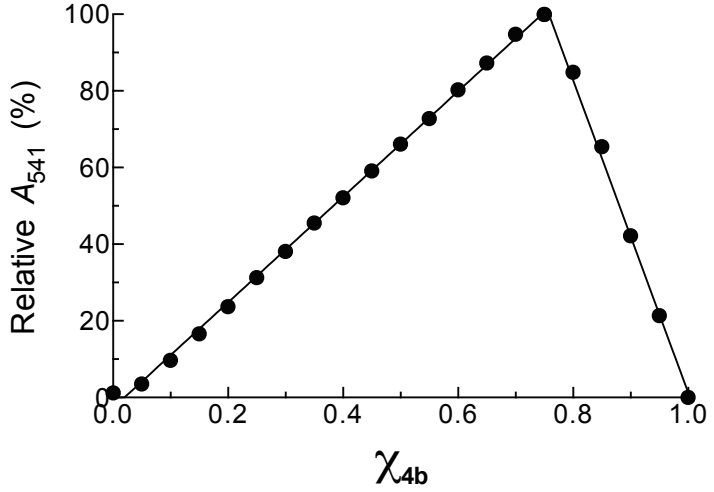

χ_{4b} at point of intersection = 0.76 ± 0.03, suggesting 3:1 (**4b**:Fe) stoichiometry

Fe(II)·(4c)$_3$

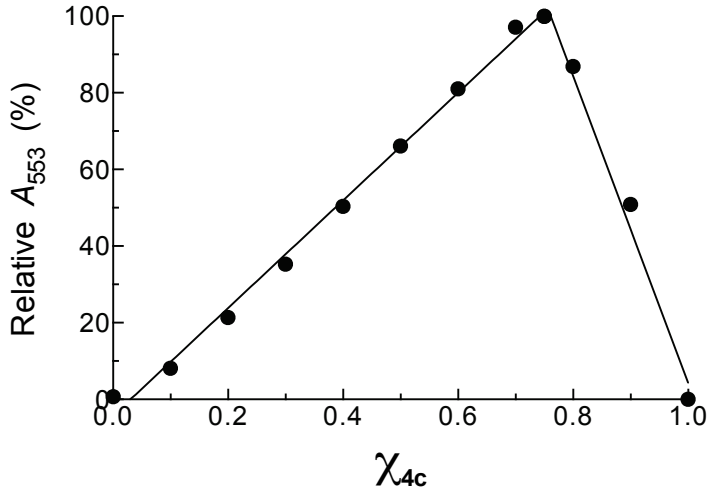

χ_{4c} at point of intersection = 0.76 ± 0.07, suggesting 3:1 (**4c**:Fe) stoichiometry

Fe(II)·(4d)$_2$

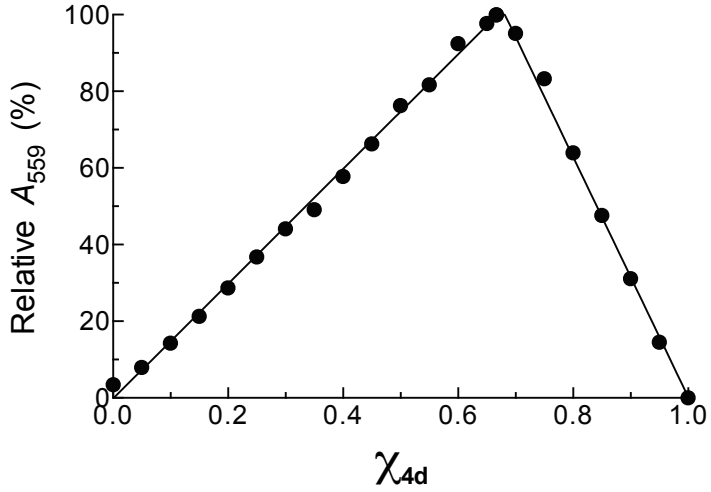

χ_{4d} at point of intersection = 0.68 ± 0.02, suggesting 2:1 (**4d**:Fe) stoichiometry

Fe(II)·(4e)$_3$

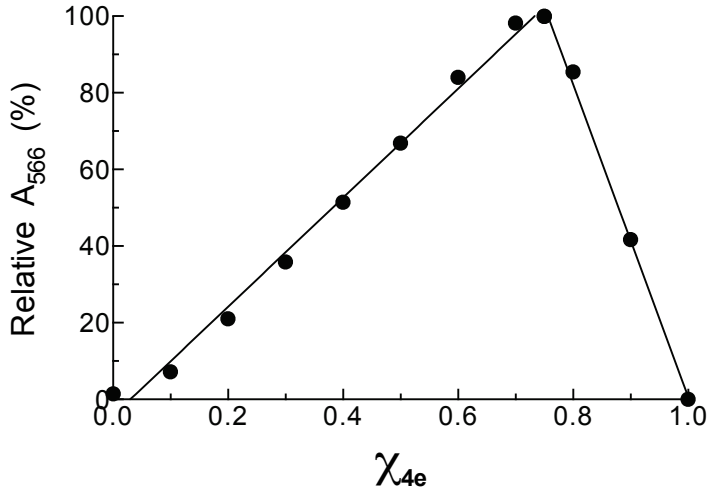

χ_{4e} at point of intersection = 0.75 ± 0.05, suggesting 3:1 (**4e**:Fe) stoichiometry

Fe(II)·(4f)$_2$

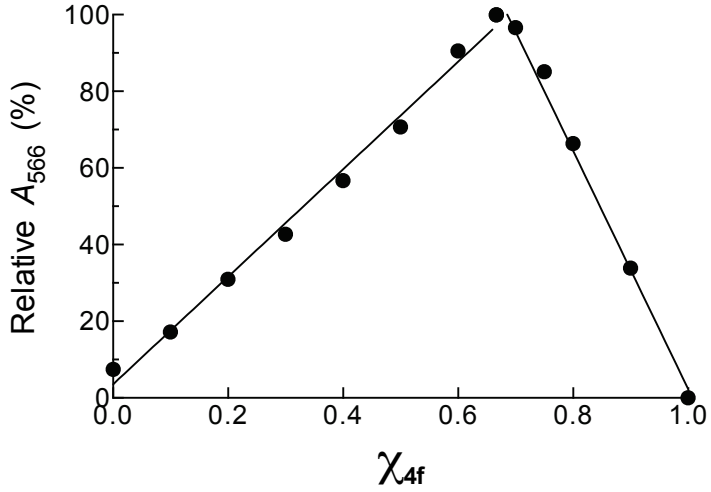

χ_{4f} at point of intersection = 0.69 ± 0.04, suggesting 2:1 (**4f**:Fe) stoichiometry
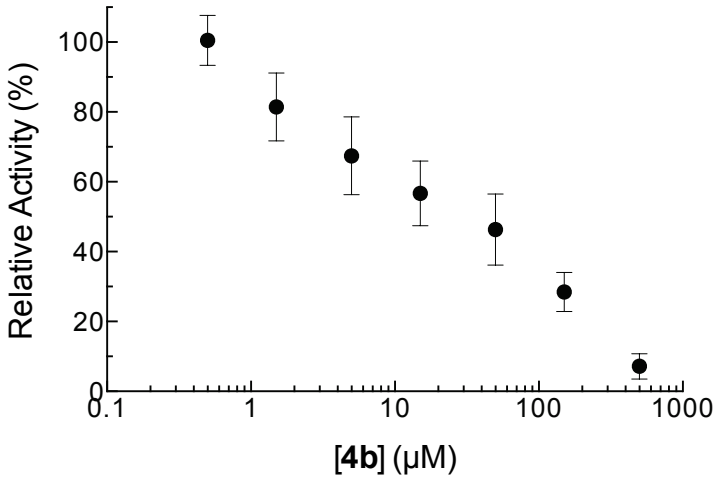
VI. Dose–response curve for inhibition of human CP4H1 by compound 4b